PRINCIPLES OF CRYSTAL CHEMISTRY

E. Cartmell

tute of Chemistry

APHS FOR TEACHERS NUMBER 18

ROYAL INSTITUTE OF CHEMISTRY
MONOGRAPHS FOR TEACHERS No. 18

Principles of Crystal Chemistry

E. CARTMELL, BSc, FRIC

Deputy Director of Laboratories in the Department of Chemistry, University of Southampton

LONDON: THE ROYAL INSTITUTE OF CHEMISTRY.

Monographs for Teachers

This is another publication in the series of Monographs for Teachers which was launched in 1959 by the Royal Institute of Chemistry. The initial aim of the series was to present concise and authoritative accounts of selected, well defined topics in chemistry for the guidance of those who teach the subject at GCE Advanced level and above. This scope has now been widened to cover accounts of newer areas of chemistry or of interdisciplinary fields that make use of chemistry. Though intended primarily for teachers of chemistry, the monographs have proved of great value to a much wider readership, including students in further and higher education.

First published June 1971

Published by The Royal Institute of Chemistry, 30 Russell Square, London WC1B 5DT, and distributed by The Chemical Society Publications Sales Office, Blackhorse Road, Letchworth, Herts SG6 1HN.

Printed by Alden and Mowbray Ltd., Oxford.

CONTENTS

1. An Introduction to Crystallography

Socrates discusses how far a flea can jump, we discuss why snowflakes, when they first fall, always have six corners and six projections, tufted like feathers. J. Kepler (1611)

The Greek word, *krystallos*, was used to describe both ice and a form of quartz known as rock crystal. This rock crystal was found in mountainous regions where the snow was intensely frozen and was evidently regarded as a special form of ice. It seems strange that the Greeks, who were so keenly interested in discussing form and symmetry, did not leave any records concerned with crystal shapes and symmetries, other than an attempt by Plato to correlate structure and properties by linking four of the regular Platonic solids—tetrahedron, octahedron, cube, and icosahedron—with the Empedoclean elements, fire, air, earth and water. Thus, he associated rock crystal with cubes of earth. In later times the association of these geometrical ideas with those of the atomists (Leukippos, Demokritos, Lucretius) provided a foundation for theories of the structure of matter developed in the 17th and 18th centuries.

A different approach can be traced back to Aristotle's discussions of matter and form and the association of fire, air, earth, and water with the 'qualities' hot–dry, hot–moist, cold–dry, and cold–moist. These ideas became linked with animistic notions concerning minerals and crystal structure, and a belief that crystals were living organisms growing by some kind of vegetative process persisted from antiquity into the age of alchemy. Lingering traces of this idea can still be found in the association of crystals with the occult. The vegetative theory of crystal growth was weakened by the work of N. Steno (1638–1686)—anatomist, physiologist, geologist, and bishop—who explained crystal growth as a deposition of particles on the faces of existing crystals from the surrounding fluid, and who also initiated the study of crystal angles.

Crystals of the same substance may have very different external forms, which arise, as is now known, from the different rates at which faces grow. Steno examined crystals of quartz which, in the ideal state, would have the form shown in *Fig. 1a*, *i.e.* a hexagonal prism capped by hexagonal pyramids. He cut sections through different specimens in planes normal to the vertical axis, and traced the cross-sectional outline to get figures of the type shown in *Fig. 1b*. These

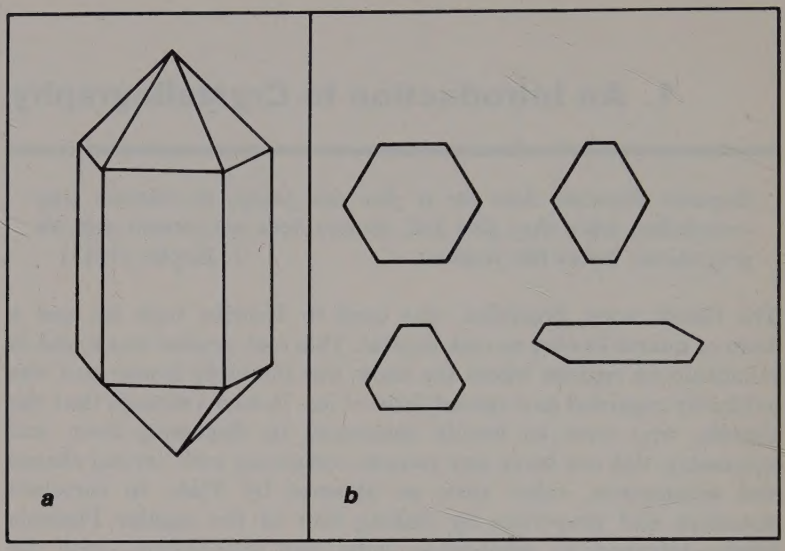

FIG. 1. Steno's drawings of quartz crystals (*a*) ideal form, (*b*) cross-sections normal to vertical axis.

sections were only rarely regular hexagons, but Steno noted that the angle between adjacent vertical faces was always 120°, irrespective of the relative face development. This work was the precursor of the *law of constant angle*, which states that the angles between corresponding faces of all crystals of the same substance have a constant value.

A much more rapid accumulation of crystal angle measurements became possible after the invention of the contact goniometer in 1780 by A. Carangeot (1742–1806). This simple device consisted of two straight edges so pivoted that they could be arranged to lie in contact with two crystal faces. The angle between the straight edges could then be measured on a protractor. A simple contact goniometer can be constructed from two pivoted strips of Meccano with a protractor bolted to one of them, as shown in *Fig. 2*.

Crystal angles are now measured very accurately by the optical goniometer invented by W. H. Wollaston (1766–1828) in 1809. The crystal is mounted so that a selected face receives a parallel beam of light from a collimator. The beam reflected from this face is observed in a suitably arranged telescope and the crystal is then rotated until the reflected ray from a second face lies in the same direction. The principle is the same as in the experiment to measure the angle of a

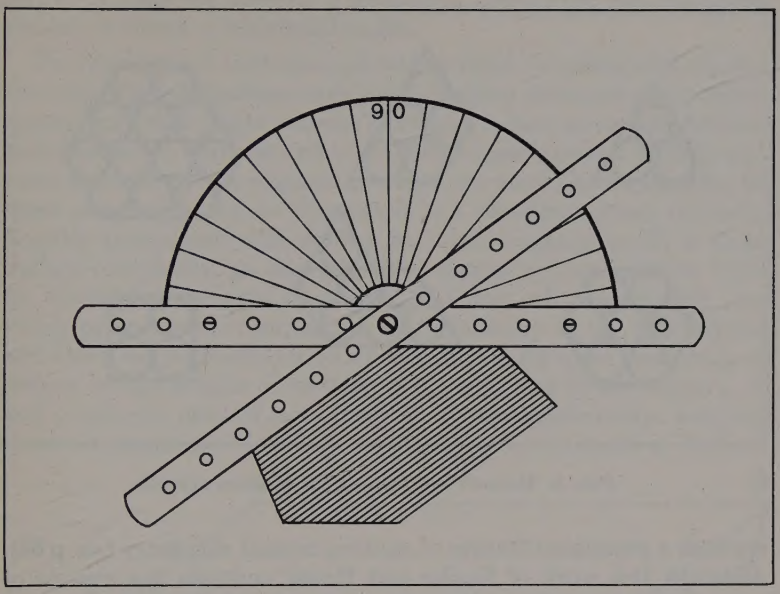

FIG. 2. A simple contact goniometer.

prism which is performed in many practical physics courses, and an extension of this experiment to relate it to crystal angles would be valuable in schools where chemistry and physics courses are well integrated.

An essential clue to the internal structure of crystals was clearly illustrated by R. Hooke (1635–1703) in his *Micrographia* (1665). He observed the different figures into which spherical shot collected when they were allowed to roll on an inclined plane and suggested that these could reproduce the known external forms of alum crystals: ' . . . by these kinds of texture or positions of globular bodies you may find out all the variety of regular shapes into which the smooth surfaces of Alum are formed . . .'. Some of Hooke's drawings are reproduced in *Fig. 3.*

A somewhat similar idea had been put forward by J. Kepler (1571–1630) in his essay on snowflakes published in 1611. He discusses the geometrical implications of structures such as the bees' honeycomb and the cells of the pomegranate and this leads him to the general problem of space-filling. Kepler illustrates the shapes that can be obtained by packing spheres in different ways, and distinguishes between the cubic and hexagonal close-packed forms which

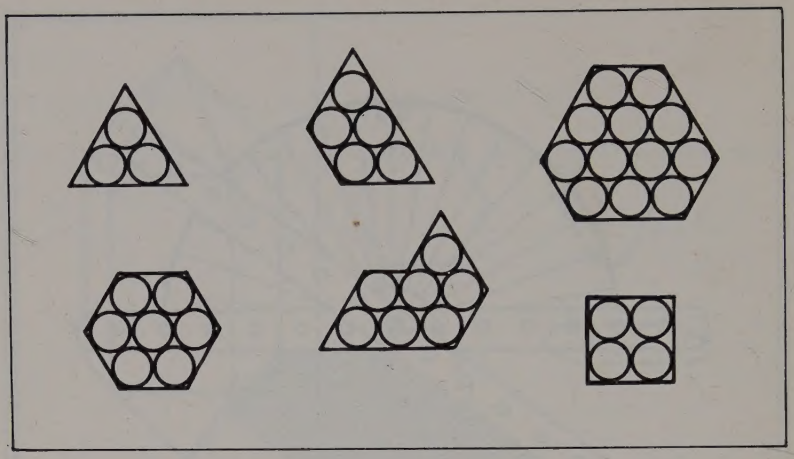

FIG. 3. Hooke's representations of alum crystals.

are such a prominent feature of modern crystal chemistry (*see* p 52). Although this work of Kepler and Hooke contains the essence of crystallography in that it discusses external form in terms of internal regularity, it is much too general to provide an adequate description of the great variety of shapes exhibited by crystals. D. Guglielmini (1665–1710) suggested that crystals are constructed by packing small *polyhedral* units closely together—an idea that was supported by the work of R. de l'Isle (1736–1790) and his pupil Carangeot. Credit for the polyhedral theory is, however, usually given to the Abbé Haüy (1743–1822), professor of mineralogy in the University of Paris and honorary canon of Notre Dame. One of the picturesque stories of science concerns Haüy's visit to a friend who owned a fine collection of minerals. Haüy accidentally dropped a splendid specimen of calcite, but noted that the resulting debris contained small rhombohedral units, whereas the original specimen had the characteristic form in which the calcite crystals are terminated by pyramidal faces. This accident is said to have supplied the inspiration for Haüy's theories of crystal structure based on packing small units such as the rhombus to fill space completely. Haüy may well have dropped the calcite specimen, but the description of its structure in terms of a regular arrangement of polyhedral units had been common currency in scientific circles for many years. Thus, C. F. Westfield (1746–1823) in 1767 discussed calcite crystals as assemblies of rhombohedral cleavage fragments. Haüy's great achievements were to use this idea of regular stacking of polyhedral units to work out precise values for the angles between prominent crystal faces,

and to provide the basis for a method of identifying and classifying crystals in terms of interfacial angles.

The requirement that space should be filled completely by regular stacking of small identical units puts a limit to the number of possible types of unit that can be chosen. There are, in fact, seven possibilities, and these seven *unit cells* define the seven *crystal systems*. (The limitations imposed by the requirement that the units should stack to fill space completely can be illustrated in a two-dimensional example. Regular pentagonal tiles cannot be fitted together to fill a plane surface completely, so that five-sided figures are not possible units for developing a crystal structure.) The unit cell, the smallest unit which preserves the composition and symmetry of the bulk crystal and which can be stacked with similar units to fill space completely, is defined by the lengths of its sides, a, b, and c, and by the angles α, β, and γ between pairs of sides (*see Fig. 4*). The relationships between these six parameters define the crystal system, as set out in Table 1.

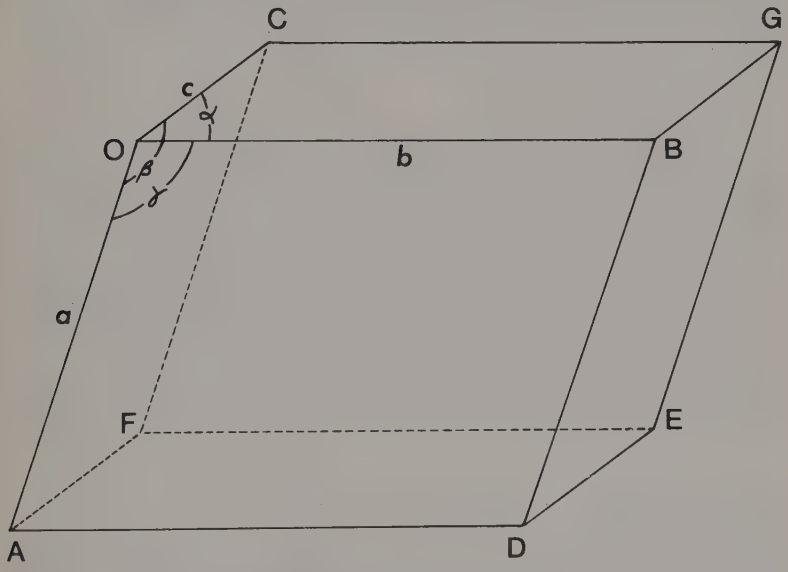

FIG. 4. The unit cell.

Table 1. The crystal systems

Cubic	$a=b=c$	$\alpha=\beta=\gamma=90°$
Tetragonal	$a=b$; c	$\alpha=\beta=\gamma=90°$
Orthorhombic	a; b; c	$\alpha=\beta=\gamma=90°$
Rhombohedral	$a=b=c$	$\alpha=\beta=\gamma$
Hexagonal	$a=b$; c	$\alpha=\beta=90°$; $\gamma=120°$
Monoclinic	a; b; c	$\alpha=\gamma=90°$; β
Triclinic	a; b; c	α; β; γ

The further developments of classical crystallography were concerned with crystal symmetry and the space lattice. We have already seen that crystals of the same substance (*e.g.* quartz) may have different external forms or *habits*. Sodium chloride provides another example; small cubes are obtained on crystallization from aqueous solution, but octahedral crystals are obtained if urea is added to the crystallizing solution. Both forms have the same cubic unit cell but they are distinguished by different symmetry properties. Sodium chlorate provides another good example. It normally grows as cubic crystals, but may appear as tetrahedral units if borax is added to the solution from which it is crystallizing. The unit cell classification of crystal structure was extended (mainly by Victor von Lang) to assign crystals to one of 32 crystal classes, differentiated by their *symmetry elements*.* These elements are the centre of symmetry, mirror planes and rotational axes. A symmetry operation linked with these elements—inversion through a centre, reflection in a plane, rotation by a defined angle about an axis—converts the crystal into a form indistinguishable from that which it possessed before the operation was carried out.

Inclusion of two further symmetry elements which become possible in three-dimensional crystal structures—glide planes and screw axes—produces 230 possible combinations called *space groups*. It is rather remarkable that the working out of these possibilities was achieved almost simultaneously from about 1890–1895, by three men working independently in very different parts of Europe—E. S. Federov, a Russian crystallographer and mineralogist, A. M. Schönflies, a German mathematician, and W. Barlow, an English businessman and amateur man of science. Assignment of crystals to their appropriate space groups is an essential step in the determination of structure by x-ray diffraction methods, but is not essential in a discussion of crystal chemistry at the level we are concerned with.

The space lattice

It is mathematically convenient to discuss unit cells and crystal structure in an abstract way by linking them with a three-dimensional array of points called a space lattice. The development of a lattice array is illustrated in *Fig. 5*. A point O is chosen as origin and three axes OA, OB, and OC are defined. A line of points along the axis OA with equal spacing a defines a lattice row. Similar parallel rows

* Excellent discussions of symmetry elements and operations will be found in the books by Phillips and Wheatley (*see* Suggestions for Further Reading p 00).

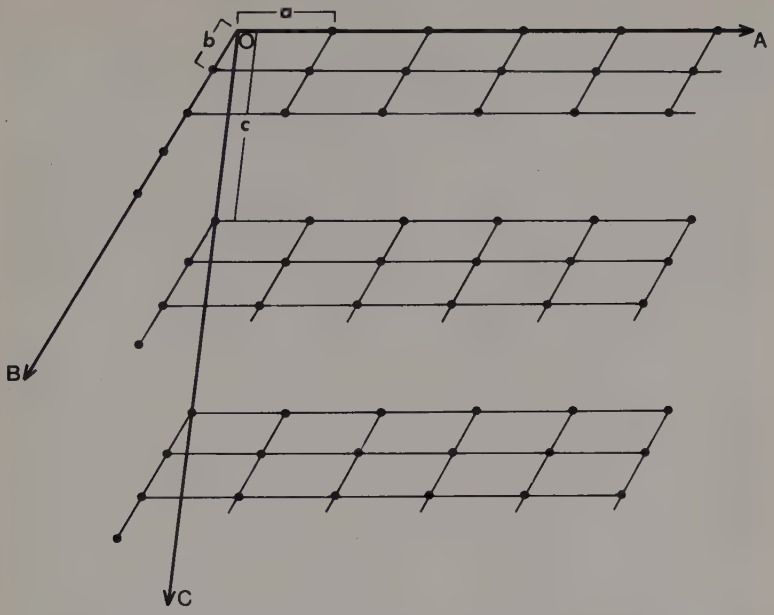

FIG. 5. The space lattice.

originating from points along OB with equal spacing b produce a two-dimensional net, and parallel nets originating from points at spacing c in OC develop the full three-dimensional lattice array. The lattice so formed is defined as an array of points such that the environment of any one point is the same in arrangement and orientation as that of any other point in the array.

FIG. 6. Possible unit cells.

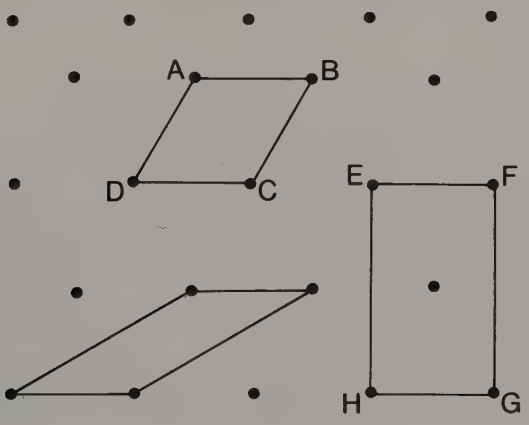

Figure 6 represents a two-dimensional space lattice on which a number of unit cells have been drawn. Some units are larger than others, and it is often convenient to choose that which has the smallest area (or volume, in three dimensions)—*e.g.* ABCD in *Fig. 6*. Geometrical considerations may also influence the selection of a unit cell. Relationships between unit cell dimensions and the spacing between various sets of parallel planes going through lattice points are much simpler if unit cell angles are right angles. Thus in the lattice shown, it might be that a cell such as EFGH would be a better choice. This differs from ABCD in that, in addition to points at the corners of the unit cell, there is an additional point at the cell centre.

A lattice produced from a unit cell of type ABCD with lattice points at the cell corners is called a *primitive* or *P*-type lattice. There are, therefore, seven *P*-type lattices associated with the seven crystal systems. In addition to these *P*-type lattices there are other, rather more complex types. Thus the primitive lattice in the cubic system can be supplemented by a *face-centred* or *F*-type lattice, with points at the centres of the six cube faces as well as at the eight corners, and the *body-centred* or *I*-type lattice with a point at the cube centre as well as the eight at cube corners. (The designation *I* comes from the German word for body-centred—*innenzentrierte*). *Figure 7* illustrates these lattice types. The *F*- and *I*-type lattices can always be

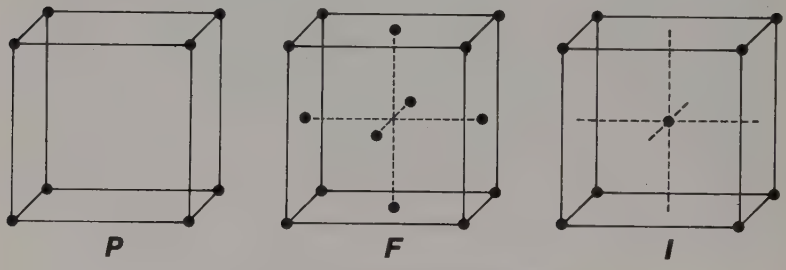

FIG. 7. *P*-, *F*-, and *I*-type lattices.

derived from a primitive unit cell with points at the corners only, but *Fig. 8* shows that the *P* lattice is less symmetrical than the *F*- or *I*-types and less suitable for calculations relating unit cell dimensions to possible spacings of sets of parallel planes in the lattice. A. Bravais (1811–1863) showed that fourteen lattices were possible when *P*, *F*, *I*, and *C* (lattice points at the centres of one opposite pair of faces) arrangements were considered. At first sight it would seem that there should be more possibilities than this, but in some of the seven crystal systems there are only two different Bravais lattices and in others only one. For example, *Fig. 9* shows two unit cells of a tetragonal

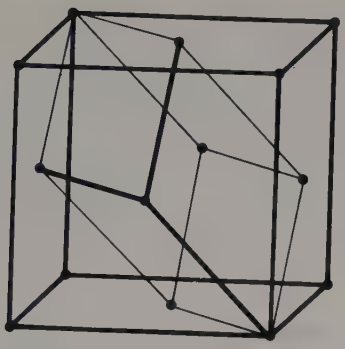

FIG. 8. The relationship between F- and P-type lattices.

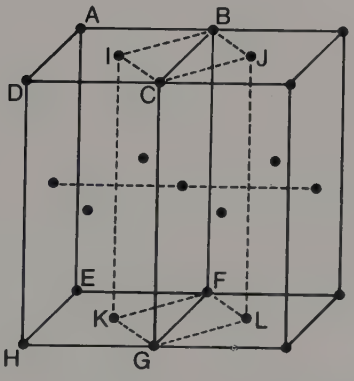

FIG. 9. F and I unit cells in the tetragonal system.

lattice. This lattice can be derived equally well from the face-centred unit ABCDEFGH or the body-centred unit IBJCKFLG. Diagrams of the 14 Bravais lattices are given in the standard texts quoted in the bibliography (p 68). At the level of this work, however, we need only be concerned with the P, F, and I lattices of the cubic system.

It should be emphasized at this stage that the space lattice is a mathematical abstraction—an array of points. Nothing has been said so far about the positions of the atoms of a crystal with respect to these points. Atoms need not be situated on lattice points but it is often convenient to choose an atom or ion as the origin of the lattice. In the case of metal structures in particular this often results in the location of other atoms or ions on lattice points. Thus the atoms (or

ions) in the structure of gold are located on the points of an F-type cubic lattice whereas those of α-iron form an I-type cubic lattice. We shall see later (*e.g.* p 43) that many simple inorganic compounds have structures in which lattice points are the sites for atoms or ions, but the atoms of large organic molecules may not be on lattice points at all. However, if the positions of the atoms within a unit cell can be determined, the crystal structure is then also determined, since the unit cell must possess the composition and the symmetry of the bulk crystal formed by stacking identical units together.

The law of rational indices

Figure 10 represents a two-dimensional crystal in which O is chosen as an arbitrary origin, and OA and OB as appropriate axes. The sides of the unit cell, OA and OB, are of lengths a and b respectively, and the angle between them, $AOB = \gamma$. These axes, OA and OB, will normally be chosen in directions parallel to prominent crystal planes. Removal of unit cells in a regular way may produce new faces. CD, for example, represents a direction parallel to one of these new faces. If we now draw lines parallel to CD through all the lattice points, we shall get a set which makes intercepts on the sides of the unit cell defined by OA and OB. We now select the line which is nearest to the origin O and note that it makes an intercept of length $a/1$ on OA, and an intercept of length $b/2$ on OB. We can extend this construction to three dimensions. *Figure 11* represents a unit cell, defined by the sides OA ($=a$), OB ($=b$), and OC ($=c$), and XYZ represents a plane selected as the one nearest to the defined origin in a set, all of which are parallel to a given crystal face. The intercepts made by this plane on OA, OB, and OC will be, in general, a/h, b/k, and c/l res-

Fig. 10. Sets of parallel planes in a two-dimensional lattice.

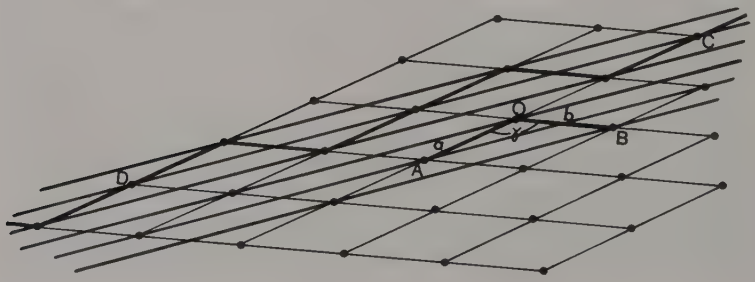

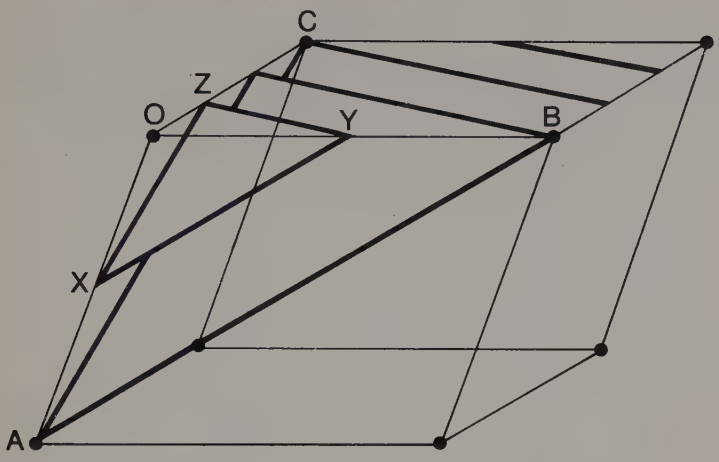

Fig. 11. Miller indices for sets of parallel planes, in this case 223.

pectively, and one way of stating the law of rational indices is that for any crystal face, h, k, and l defined in this way are small integers (usually not greater than three). Since the sets of parallel planes were obtained by drawing them through lattice points this is equivalent to saying that important planes in a crystal are those with a high density of lattice points. Planes which only go through a few lattice points will make very small intercepts on OA, OB, and OC—that is, h, k, and l would be large integers.

The three integers, h, k, l, are called the Millerian or Miller indices of the plane [after the crystallographer W. H. Miller (1801–1880)]. They are written down without interposing commas, but they are read as separate numbers, so that 321 is described as a three, two, one plane.

A plane that is parallel to one or more of the axes (say, *e.g.* OA) will make an infinitely long intercept; thus $a/h = \infty$, so that $h = 0$. The origin O will always be chosen in the interior of the crystal, so that some intercepts may be on negative axes. The Miller index is then written with a bar above it, *viz.* $\bar{3}21$. *Figure 12* shows a cubic crystal with the origin taken at the centre and principal axes OA, OB, and OC. The six faces are indexed as 100, $\bar{1}00$, 010, $0\bar{1}0$, 001, and $00\bar{1}$.

A set of equivalent faces can be described collectively by using curly brackets { }; *i.e.* {100} implies the six cube faces described in the diagram. It will be seen from *Fig. 12* that 010, $0\bar{1}0$, 001, and $00\bar{1}$ are

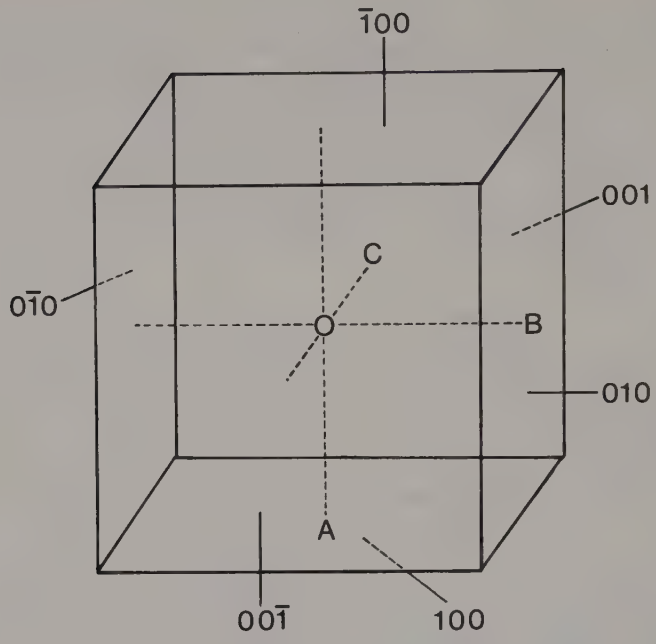

Fig. 12. Miller indices for the faces of a cubic unit cell.

all faces parallel to the OA axis. They are classified as belonging to a zone and are represented conveniently by a notation using square brackets, [010].

With the advent of x-ray crystallography, assignment of Miller indices to particular crystal faces has become of less importance. In x-ray crystallography the essential feature of crystal structure is the presence of sets of equally spaced parallel planes on which atoms are located. The Miller indices are now used to represent sets of parallel planes, rather than a particular crystal face. Thus the indices 111, 222, 333 may all be important in x-ray work. They represent sets of planes which are parallel to a particular plane labelled 111 in classical crystallography. The spacing of the 222 set is however only half that of the 111 set, likewise the spacing of the 333 set is one-third that of the 111 set. In general, when the Miller indices are used to denote sets of parallel planes, high index values imply closely-spaced planes, low values indicate planes which are relatively far apart.

This nomenclature for crystal planes is not at all necessary in elementary courses. Particular planes can easily be identified in the normal way by letters. Sooner or later, however, students will come

across diagrams with Miller indices and it is the author's experience that this method of discussing them, in terms of intercepts made by parallel planes, is accepted much more readily than that adopted in many textbooks of optical crystallography which is concerned mainly with labelling crystal faces.

2. Crystal Growth

In discussing the shapes of crystals and the geometry of unit cells we draw idealized diagrams—regular polyhedra such as the cube and the octahedron with a limited number of well-defined faces. Real crystals with shapes approximating to these ideal forms may be found in mineral collections, or they may be grown artificially under carefully controlled conditions but, in general, crystals look very different from the ideal form. Cubic crystals of sodium chloride may be obtained from a well-stirred solution, but the crystals lying on the bottom of the crystallization dish will probably have a 'tablet-shaped' appearance. Some crystals grow in thin needles; others, the so-called dendritic forms, shoot out tree-like branches. Any theory of crystal growth must give some explanation of these different external forms.

Crystals can be grown from melts, from saturated solutions (using aqueous or non-aqueous solvents) or by direct deposition from a gaseous phase on to a cooled surface. In each case, growth starts on a small nucleus. (In the discussion that follows we are going to assume that some nuclei are always present. The way in which the nuclei are formed in the first place presents some quite difficult problems which are outside the scope of this work. We recall the words of the eminent Scots divine, who in the course of a sermon said 'here, O Lord, as thou knowest, we come to a difficulty, and having looked it boldly in the face we pass on').

Crystallization in melts starts from nuclei which tend to be formed close to the walls of the mould where the rate of heat loss is greater than in the bulk material. Growth then proceeds fairly easily in a direction normal to the mould surface with the production of needle-shaped crystals. Growth parallel to the walls is, however, inhibited by mutual obstruction, and the net result is the production of a grain structure as the melt solidifies. Physical properties such as tensile strength are greatly affected by grain size, and control of this factor is an important aspect of the metallurgist's art. In general, slow cooling, which allows nuclei to be more widely dispersed throughout the melt, promotes small grain size. A similar grain structure is seen in igneous rocks such as granite which have crystallized from a silicate melt.

It should perhaps be emphasized that the geometry of these grains is not necessarily related to the structure of the individual crystals.

The grains in metals, alloys and rocks sometimes have a very regular hexagonal cross-section, and the hexagonal pillars of the Giant's Causeway and Fingal's Cave illustrate this on a grand scale. The geometry in these cases results mainly from the mechanical constraints that arise when growing crystals meet each other in a confined space.

Another factor that affects crystal growth is the requirement that new material must be brought up to the crystal surfaces to replenish the solution from which material has already been deposited. Needle-shaped growth probably arises from the fact that replenishment will occur most readily at the corners and edges of the growing crystal. Another factor is the heat or enthalpy of crystallization. Crystallization can only continue if this heat of crystallization is dispersed; otherwise there will be a temperature rise and solution of the crystal. This heat will be dispersed more readily from the edges and corners of crystals, and this will again favour needle-shaped or dendritic growths.

Mechanism of crystal growth

The essential features of crystal growth can now be discussed in relation to crystal structure. For this purpose it is not necessary to specify the precise location of atoms, ions, or molecules in the crystal structure. We can use as a model an assembly of unit cells, held together in a regular arrangement by forces arising from the particles present in each cell.

Nuclei are presumably formed in the first place by chance collisions of several units, and the probability that these units will be present simultaneously in a small volume will depend upon both concentration and temperature. Increasing supersaturation should therefore promote the formation of crystal nuclei and hence speed up the rate of growth, whereas an increase in temperature will tend to disrupt nuclei by thermal motion, with a reduction in the rate of nucleation and a corresponding reduction in growth rate.

We must now consider in more detail the way in which a new unit may attach itself to the crystal surface. *Figure 13a* represents a crystal surface. One layer, AB, has been partially covered by a new layer CD, thus forming a step or ledge at D. *Figure 13b* represents two possible ways in which a new unit might attach itself to the surface. In position (*i*), one face of the arriving unit is attached to one face of the crystal surface, whereas unit (*ii*) is in contact with two units at the step or ledge in the surface layer. In this way we get a (somewhat naïve) interpretation of the experimental observations that crystals tend to grow in surface layers—new units preferring to complete existing layers before starting new layers.

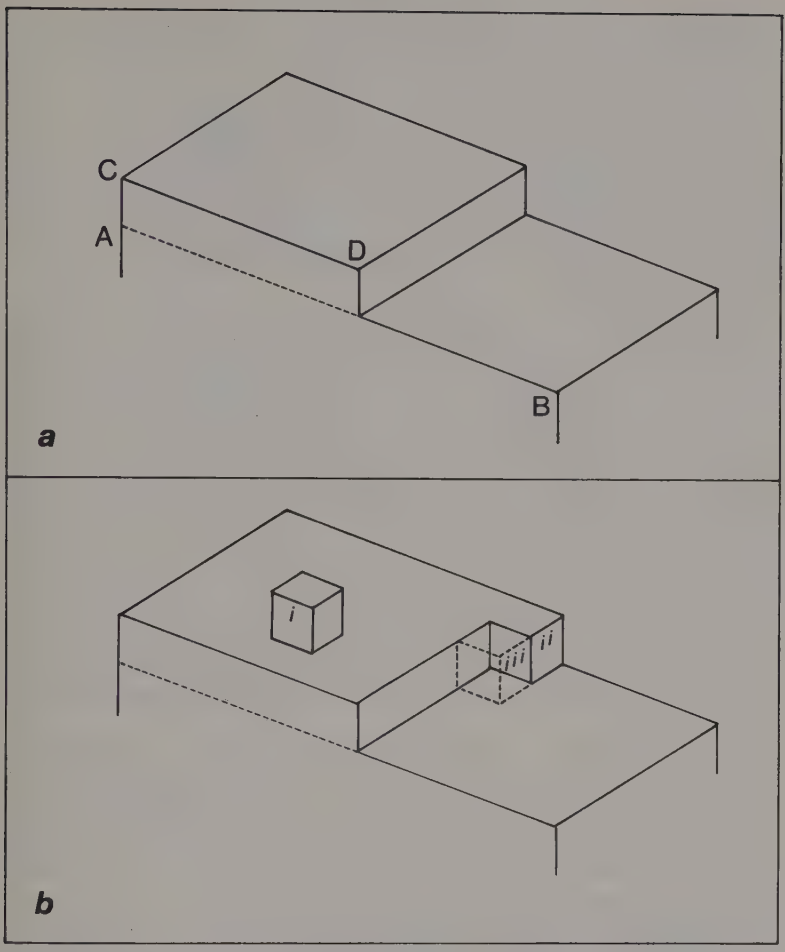

FIG. 13. Crystal growth (*a*) layer CD partially covering layer AB; (*b*) possible locations of new units arriving at the crystal surface.

A more detailed treatment of crystal growth involves consideration of free-energy changes. New material will attach itself to the surface in positions for which there is a maximum decrease in free energy for the change:

substance in solution → substance in crystalline solid

Two important factors that influence the magnitude of this free-energy change are the interaction energy between the units and the change in surface energy. This second factor is a consequence of the

fact that a unit in the interior of the crystal is completely surrounded by neighbouring units, whereas a unit in the surface layer has an incomplete environment. When a unit arrives on the surface in position (*i*) of *Fig. 13b* one face of the unit is in contact with one unit in the crystal surface, with the result that the surface area of the crystal increases by four units—the four vertical faces of the newly arrived unit. (The top surface of the new unit replaces the surface area on which it is sitting.) There is therefore an increase in surface free energy, and this will be an unfavourable factor for stable attachment to the surface.

In position (*ii*), however, two faces are in contact and the surface area only increases by two units; this produces a free-energy change more favourable for crystal growth. An even more favourable free-energy change situation arises if a new unit arrives at the ledge in *Fig. 13b* and occupies the position adjacent to unit (*ii*). There will then be three faces in contact and no net increase in surface area. Crystals can therefore grow if new material is deposited at steps in the surface until the layer is completely covered. But what happens when the layer is complete? We have already seen that there is a most unfavourable free-energy situation for a unit arriving in position (*i*) of *Fig. 13b* to start a new growth layer. It would tend to bounce off again, or be knocked off by collisions with other units in the surrounding medium. The calculated growth rate would be infinitesimally small—a result strikingly at odds with experimental observation.

One way of getting out of the difficulty is to realize that the argument has been developed for a surface of close-packed units. In fact, many crystals have surfaces that are far from close-packed. Some molecules may protrude from the surface while at other parts of the surface there may be cavities. There will therefore be many sites where an incoming unit can be attached without creating an impossibly large increase in surface free energy.

Another way out of the difficulty which accounts for growth on close-packed surfaces was suggested in 1949 by F. C. Frank. He pointed out that real crystals are not perfect or ideal structures, and that certain types of defect in the crystal structure could provide a mechanism whereby steps or ledges in the surface are continuously created. New material arriving at the surface would then always find a ledge on which to anchor. The particular defect which provides this haven is called a *screw dislocation*, defined as follows.

Figure 14a represents a crystal lattice into which a vertical cut in the plane ABCD has been made. If the lattice is sheared along the cut in the directions shown by the arrows a dislocation is produced as shown in *Fig. 14b*. The line AB is called the axis of a screw disloca-

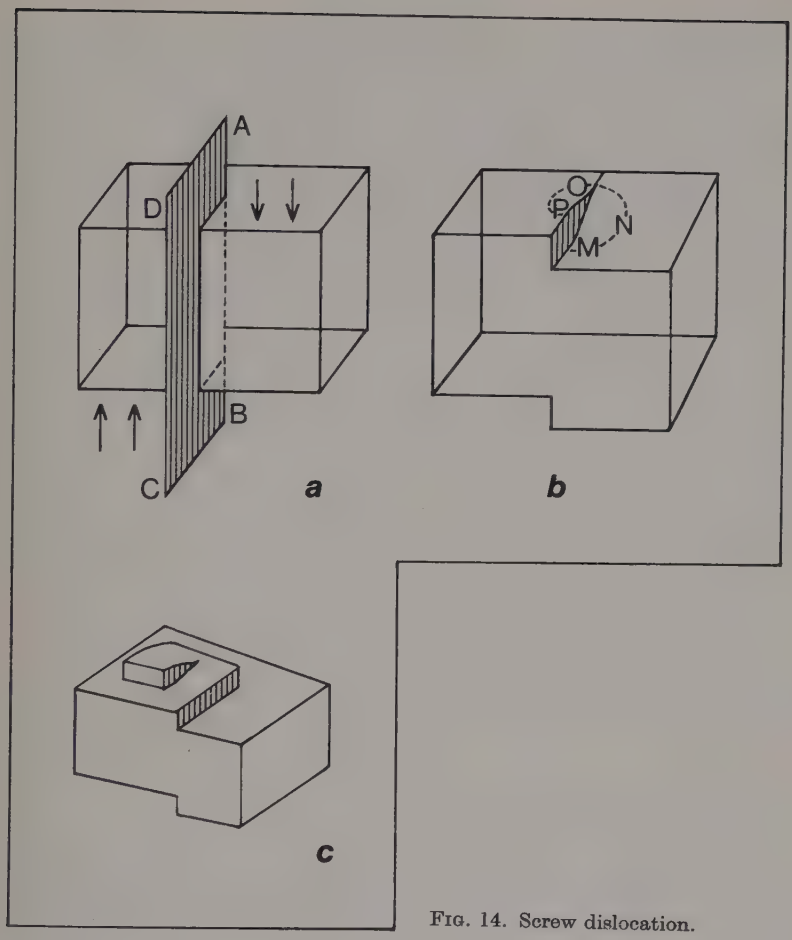

FIG. 14. Screw dislocation.

tion since it effectively converts a multilayer crystal structure into a single-layer 'ramp' spiralling around the axis AB. A journey from point M in the lattice to a point P vertically above it can be made along the circuit MNOP without jumping over a step or starting an entirely new layer. The helical ramp formed by the addition of new material is shown in *Fig. 14c*. Spiral development of crystal faces was in fact observed experimentally by both electron microscope and optical microscope examination of crystal surfaces shortly after Frank had published his theory.

Students often find it difficult to visualize the formation of a

growth spiral from a two-dimensional diagram. A very convenient model can be made by using sugar cubes as the constructional units for the crystal structure (the wrapped variety has a slightly smaller wastage rate). A cardboard wedge can be inserted under a portion of a stack of cubes to provide the dislocation. New units can then be added at the ledge which winds round the dislocation axis which can be defined by removing a column of cubes from the centre of the stack.

3. The Discovery of x-Ray Diffraction

Munich in 1912 seems now to have provided an ideal conjunction of time, place and persons for the discovery of the diffraction of x-rays by crystals. Some of the people concerned, in particular A. Sommerfeld, Max von Laue and P. P. Ewald, were members of a group of physicists who frequently adjourned after lunch to the Café Lutz near the Hofgarten in Munich, and it was here that a chance remark by Ewald gave von Laue the idea that crystals might act as a diffraction grating for x-rays. Elementary textbooks of chemistry and physics often state that von Laue, with the assistance of his research students, observed the effect of allowing a beam of x-rays to fall on a crystal of zinc blende. The rays leaving the crystal were intercepted by a photographic plate which, on development, revealed a symmetrical pattern of spots demonstrating that the x-rays had been diffracted. Statements like this represent rather less than the truth. The first crystal diffraction experiments were done with copper sulphate, and the first plates to be developed showed no signs of any diffraction effects at all. Fortunately, however, some of the people linked with this story are still alive, and they have recorded their impressions of what in fact happened.

In 1912 the great wave of new discovery in atomic physics, launched by J. J. Thomson with the electron theory, was still sweeping forward with a splendid momentum. The discovery of radioactivity and of x-radiation in the closing years of the 19th century had been closely followed by the revolutionary quantum theory of Max Planck in 1900. One of the keenly debated questions concerned the nature of the x-rays. These rays were produced from discharge tubes not unlike those used for the production of cathode rays, many of the properties of which are also possessed by x-rays (*e.g.* ability to ionize gases by collision). At the same time, investigators from Röntgen onwards were strongly inclined to support a 'wave' hypothesis for the radiation, and they realized that an experimental demonstration of x-ray diffraction effects would be required. Some particularly thorough experiments were devised and carried out by Sommerfeld, professor of physics in Munich, in 1912. He was not able to detect any diffraction effects, but he was careful to point out that his failure did not necessarily disprove the wave theory of x-radiation, but showed, rather, that if x-rays were electromagnetic radiations, they

must have a very small wavelength (*ca* 10^{-10} m). Any longer wavelengths should have given diffraction effects with the equipment he was using.

Von Laue had come as a lecturer to Munich from Berlin in 1909, attracted by the strong school of theoretical physics that Sommerfeld was building up. During part of 1911 and early 1912 he was working on a chapter concerning wave optics in a many-volume encyclopaedia for which Sommerfeld was one of the editors. He was, therefore, immersed in the classical theories of light diffraction at a time when the possible diffraction of x-rays must frequently have been discussed. Ewald was concerned with some purely mathematical problems in crystal optics, and a discussion with him reminded von Laue that classical crystallography was based on the assumption of an internal regularity in the crystal structure. Nothing was then known in detail about this internal regularity, but by using some recent measurements of the Avogadro number by Perrin and by Millikan together with the value of the density of a crystal such as diamond von Laue was able to work out a value for the 'atomic volume' of carbon atoms in diamond. The distance between the atoms could then be determined if close packing of carbon atoms in diamond was assumed. This rough calculation gave a value of about 2×10^{-10} m for the distance between adjacent atoms, a value which Sommerfeld had suggested already for the wavelength of x-rays, if they were indeed electromagnetic waves.

The development of the story now takes us from the Café Lutz in Munich to the Bavarian Alps. Sommerfeld, Wien, von Laue and a few other physicists were in the habit of taking a ski-ing holiday in the Easter vacation. The proposed experiment—diffraction of x-rays by regularly placed atoms in a crystal—was much discussed, and both Sommerfeld and Wien (two very distinguished professors) decided that there were no prospects of success. Their main objection, a very reasonable one, was that the thermal motion of the atoms would destroy the regularity essential for the diffraction effect. (It is now known that thermal effects do have a profound influence on the diffraction intensities, but they do not destroy the pattern completely.)

Fortunately, however, the group contained two young research workers with sufficient enthusiasm to try the experiment even though there was little encouragement to do so—von Laue's research assistant, W. Friedrich, and P. Knipping, one of Röntgen's research students. The only x-ray machine available was a not very powerful medical set, and they anticipated that exposures of at least 10 hours would be needed to record any diffraction effects. It is hard to appreciate today, when x-ray outfits can be bought over the counter, that

to keep an x-ray tube running for 10 hours in 1912 required experimental skill of the highest order.

They chose a copper sulphate crystal for their first experiment, partly because it was a crystal that even a department of physics might have around the place, but mainly for a good scientific reason. It was well known in 1912 that when copper was irradiated with x-rays, so-called 'secondary' x-rays were emitted by the copper. Friedrich and Knipping therefore assumed that diffraction effects would most likely be observed from the secondary x-rays emitted from regularly spaced copper atoms in a copper sulphate crystal exposed to a primary beam. They arranged a photographic plate between the x-ray tube and the crystal, a position which seems strange to us, but one which seemed the only logical one in the light of what was known in 1912. No diffraction effects were observed, and it was only when they put the photographic plate in what was to them a most unfavourable position on the far side of the crystal from the x-ray tube that diffraction effects were recorded for the first time.

Von Laue heard the news of the successful experiment and worked out the theory of the effect—three fold diffraction by linear gratings. It now became easy to get facilities for further experiments. A new and more powerful x-ray tube was presented, and soon beautifully symmetrical diffraction patterns from zinc blende crystals were obtained.

Two new fields of study of far-reaching importance—x-ray spectroscopy and x-ray crystallography—came into being with the success of the von Laue, Friedrich and Knipping experiment.

The early development of x-ray crystallography was to take place very largely in Great Britain through the work of W. H. and W. L. Bragg. Von Laue himself was content with the knowledge that the experiment worked. He left Munich for Zurich in December 1912 and in later years he said he could never understand the excitement produced by the demonstration of x-ray diffraction by crystals. He always regarded it as a demonstration of the obvious.

The rapid development of x-ray crystallography stemmed from W. L. Bragg's treatment of the diffracted rays as reflections from parallel planes of atoms in the crystal structure. This theory, combined with results obtained with the x-ray spectrometer designed by his father, W. H. Bragg, enabled them to work out, during the years 1912–14, the structures of substances such as sodium chloride, potassium chloride, zinc blende, iron pyrites, and diamond. This had an immediate impact on chemistry. The structure of sodium chloride, for example, showed that there were no molecules of NaCl but that each atom of sodium had six chlorine atoms around it at equal dis-

tances, and each chlorine had six sodium atoms around it. (The subsequent development of the electronic theory of valency from 1916 onwards showed that the structural units were ions rather than neutral atoms). The diamond structure, in which each carbon atom has four nearest neighbours tetrahedrally disposed around it, provided the starting point for the very many subsequent structure determinations of carbon compounds.

The development of quantum chemistry from 1925 onwards introduced the concept of charge density, *i.e.* electronic charge per unit volume, into chemistry and development of the Fourier analysis method of structure determination enabled the x-ray crystallographers to compute this charge density at given points within the unit cell from the positions and intensities of diffracted beams. The results are normally illustrated by contour diagrams—lines of constant electron density. *Figure 15* shows one such diagram for sodium

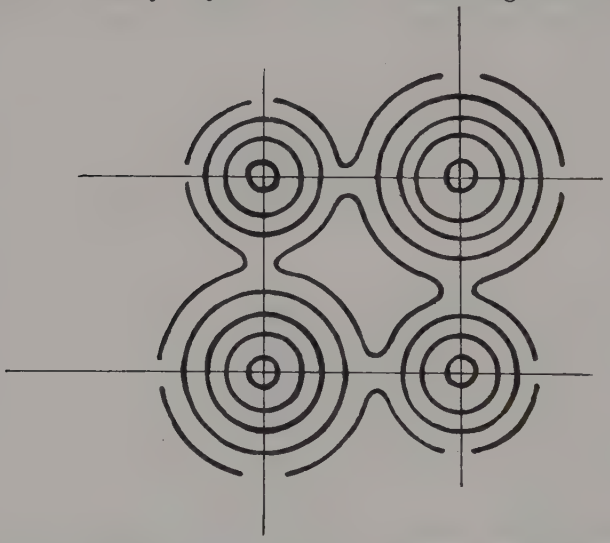

Fig. 15. Electron density contours for sodium chloride (after W. Witte and E. Wölfel).

chloride in which the contour lines are concentric circles centred on the sodium and chorine nuclei. The density increases to a maximum at each nucleus but falls to a minimum value in the region between the nuclei. A boundary surface can be drawn around each so that the structure becomes a three-dimensional one of spheres in contact with each other. The total amount of charge within each sphere can be calculated, and for sodium chloride it approximates to that expected for Na^+ and Cl^- ions.

The Fourier method, unfortunately, is not of general applicability and it becomes less reliable when applied to heavier atoms. It has been outstandingly successful for organic compounds in which the important atoms are light elements such as carbon, nitrogen and oxygen.

4. Crystal Lattice Energy

By the year 1918 the structures of a number of simple compounds had been worked out from x-ray diffraction experiments. Many of these structures (*e.g.* the alkali-metal halides) could best be considered as regular arrangements of ions, and the cohesion of the solid compounds was attributed to electrostatic interactions between these ions according to the Coulomb law. M. Born and his collaborators developed a theory of ionic crystals from 1918 onwards. and the applications of this work have proved to be extremely useful for chemistry in general and inorganic chemistry in particular.

Lattice energy is defined as the energy liberated when one mole of gaseous cations and one mole of gaseous anions are brought together from infinite distance apart to their equilibrium position in the crystal lattice at 0 K, *i.e.* the change in internal energy, ΔU, for the reaction

$$M^{z+}(g) + X^{z-}(g) \rightarrow MX(solid)$$

(Some authors define lattice energy as the increase in internal energy resulting from the separation of ions from their position in the crystal to infinite separation: this will give a different algebraic sign. The equation defining ΔU should always be quoted, otherwise arithmetical errors in crystal energy calculations are easily made.) Lattice energy can be calculated for structures consisting of spherical ions. The interaction energy between two ions of charge z^+e and z^-e separated by a distance R is, according to the Coulomb law, $-z^+z^-e^2/R$ (in cgs units; or $-z^+z^-e^2/4\pi\epsilon R$ in SI units). *Figure 16* shows part of a sodium chloride structure. Consider the interaction energy between a particular cation C and all other ions in one mole of crystalline NaCl. In this structure C has

6 nearest neighbours (Cl^-) at a distance R,

12 second neighbours (Na^+) at a distance $\sqrt{2}R$,

8 third neighbours (Cl^-) at a distance $\sqrt{3}R$,

6 fourth neighbours (Na^+) at a distance $\sqrt{4}R$, *etc.*, *etc.*

so that the Coulombic interaction energy at C becomes,

$$-(6z^+z^-e^2/R)+[12(z^+)^2e^2/\sqrt{2}R]-(8z^+z^-e^2/\sqrt{3}R)+[6(z^+)^2e^2/\sqrt{4}R]\ldots$$

or $$-z^+z^-e^2/R\times[6-(12z^+/(\sqrt{2})z^-)+(8/\sqrt{3})-(6z^+/2z^-)+\ldots]$$

The ratio of the ionic charges is constant for a given structure, (*e.g.* $z^+/z^-=1$ for NaCl, 2 for TiO_2), so that the Coulombic energy

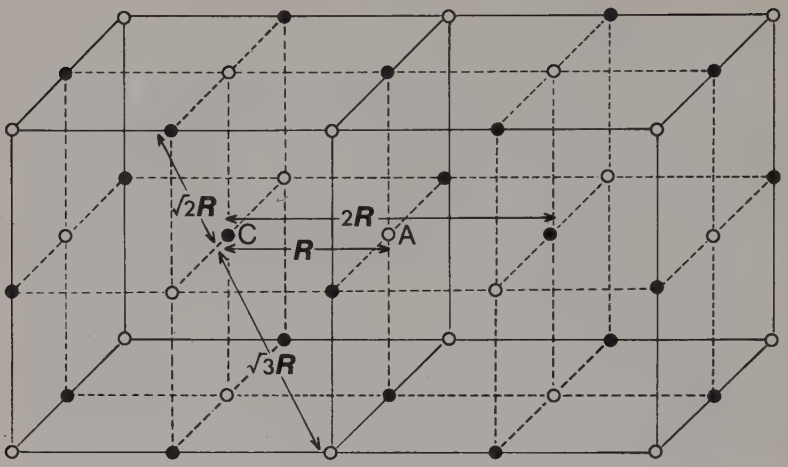

FIG. 16. The sodium chloride structure; closed circles, Na^+; open circles, Cl^-.

term can be written $U_C = -z^+z^-e^2A/R$, where A, called the Madelung constant, is written for the series enclosed within the square bracket above.

We can now repeat the analysis to get the Coulombic interaction at a particular anion A in the sodium chloride structure. This will also be $-z^+z^-e^2A/R$ since cations and anions have the same arrangement of neighbours in the sodium chloride structure. The total Coulomb energy for a lattice of N cations and N anions, where N is the Avogadro number, is then given by

$$U = \tfrac{1}{2}(U_C + U_A) = \frac{-z^+z^-e^2AN}{R}.$$

The factor $\frac{1}{2}$ is needed because $U_C + U_A$ includes the interaction between each pair.

Table 2. Madelung constants

Caesium chloride structure	1.763
Sodium chloride structure	1.748
Zinc blende structure	1.638
Wurtzite structure	1.641
Rutile structure	2.408
Fluorite structure	2.519

Madelung constants have been calculated for a large number of structures (not without difficulty) and Table 2 lists some of them. The Madelung constant is a measure of the additional interaction energy resulting from a three-dimensional lattice of ions. It may

be compared with the interaction between a single pair of ions—there is a 75 per cent increase in Coulombic energy when we go from the ion-pair $(Na^+)(Cl^-)$ to crystalline NaCl.

The Coulombic interaction energy, which represents a net attraction between the ions, must be opposed by a repulsion energy since the ions maintain an equilibrium separation in the crystal structure. A number of expressions have been suggested for this repulsion, which arises partly from the effects of overlapping charge-clouds and partly as a consequence of the Heisenberg uncertainty principle. Born and Landé first suggested the expression BN/R^n so that the lattice energy becomes

$$U = -z^+z^-e^2AN/R \quad + \quad BN/R^n$$

The constant B can be eliminated if we make use of the fact that, at $R = R_e$, the equilibrium separation of the ions in the crystal, $(\delta U/\delta R) = 0$.

This gives $$B = \frac{z^+z^-e^2A}{n} R_e^{n-1}$$

whence $$U = \frac{-z^+z^-e^2AN}{R_e}\left(1 - \frac{1}{n}\right) \text{ (cgs units)}$$

$$= \frac{-z^+z^-e^2AN}{4\pi\epsilon R_e}\left(1 - \frac{1}{n}\right) \text{ (SI units)}$$

The integer n, which depends upon the nature of the ions, can be estimated from compressibility measurements. A value of $n = 9$ is obtained for alkali-metal halide structures. Later, when the development of quantum mechanics showed that electron wave functions decreased exponentially with increasing distance from the nucleus, Born and Mayer used the expression $B'Ne^{-R/\rho}$ for the repulsion term. The constant B' can again be eliminated by putting $(\delta U/\delta R)_{R=Re} = 0$ and the expression for the lattice energy now becomes

$$U = \frac{-z^+z^-e^2AN}{R_e}(1 - \rho/R_e)$$

The constant ρ, for ions with inert-gas electron configuration, is about 0.35×10^{-10}m. A typical value of R_e is about 3×10^{-10}m, so that the repulsion term amounts to about 12 per cent of the Coulombic interaction.

In very precise calculations of lattice energy, allowance has to be made for additional interactions. Polarization of one ion by its neighbours introduces a 'dipole–induced dipole' attraction NC/R^6 (when C is an empirical constant) and the residual (or zero-point) energy—vibrational energy retained by the lattice at 0 K—must

also be included. These terms are, however, small (from 4–40 kJ mol^{-1}) compared with the total lattice energy which may be several hundreds of kilojoules per mole.

Unfortunately, Madelung constants become increasingly difficult to calculate as the complexity of the structures increases, and in recent years a semi-empirical expression for lattice energies, due to Kapustinskii, has often been used. This is

$$U = -287.2 \frac{\nu z^+ z^-}{r_+ + r_-}\left(1 - \frac{0.345}{r_+ + r_-}\right)$$

where ν is the number of ions in the formula of the substance considered (*e.g.* $\nu = 2$ for NaCl, 3 for CaF_2 *etc.*) and r_+ and r_- are the ionic radii. Values for the lattice energies of a number of crystals are quoted in Table 3 on p 32, where they are compared with values obtained indirectly from thermochemical data, using the Born–Haber cycle, which we must now discuss.

The Born–Haber cycle

There is no experimental method for the direct determination of lattice energy. A value can be obtained indirectly, however, using a method developed by Born and Haber which we will discuss using sodium chloride as an example. The enthalpy of formation of one mole of crystalline sodium chloride, NaCl(s), can be measured experimentally:

$$Na(s) + \tfrac{1}{2}Cl_2(g) \rightarrow NaCl(s);\ \Delta H = -410\ kJ\ mol^{-1}\ (298\ K)$$

This process can be broken down into a number of stages:

1. $Na(s) \rightarrow Na(g);\ \Delta H_1 = 108\ kJ\ mol^{-1}$ (298 K)
   This is the enthalpy of sublimation of sodium.
2. $\tfrac{1}{2}Cl_2(g) \rightarrow Cl(g);\ \Delta H_2 = 121\ kJ\ mol^{-1}$ (298 K)
   Here $\Delta H_2 = \tfrac{1}{2}$[enthalpy of dissociation of $Cl_2(g)$].
3. $Na(g) \rightarrow Na^+(g);\ \Delta H_3 = 489\ kJ\ mol^{-1}$ (298 K)
   ΔH_3 is the ionization potential of sodium*.
4. $Cl(g) \rightarrow Cl^-(g);\ \Delta H_4 = -365\ k\ Jmol^{-1}$ (298 K), (*i.e.* exothermic)
   ΔH_4 is the electron affinity of chlorine.*
5. $Na^+(g) + Cl^-(g) \rightarrow NaCl(s)$

---

* *N.B.* Ionization potentials and electron affinities are usually recorded in volts at 0 K. They are internal energy changes and when inserted as stages in the Born–Haber cycle the values have to be corrected to enthalpy changes (in kJ mol^{-1}) at 298 K.

ΔH_5 for this reaction* at 298 K can now be obtained by using Hess's law, since the enthalpy change for the total process, ΔH is independent of the route by which NaCl(s) is formed from Na(s) and $\frac{1}{2}$Cl(g). Perhaps the safest way to apply Hess's law is to plot enthalpies on a vertical scale in a diagram of the type shown in *Fig. 17*, where an arrow pointing upwards indicates an increase in

FIG. 17. The Born–Haber diagram for sodium chloride.

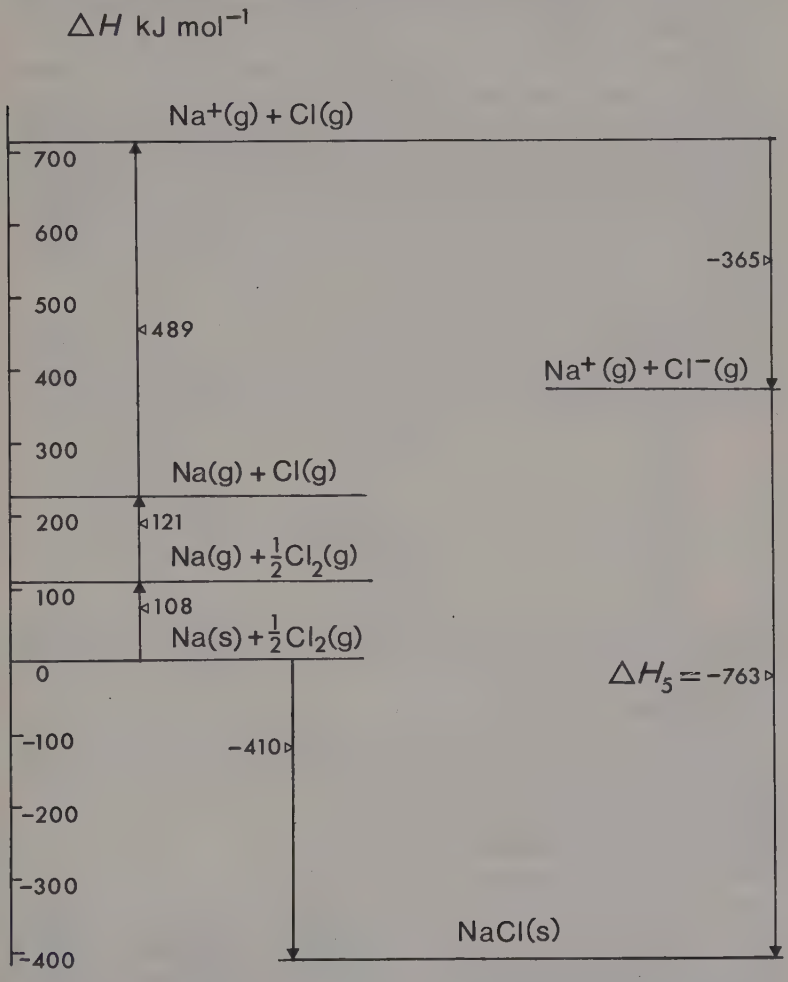

* *N.B.* The heat needed to vaporize crystalline NaCl is considerably less than the lattice energy since there is an appreciable concentration of ion-pairs, Na^+Cl^-, at temperatures just above the boiling point of NaCl.

enthalpy (ΔH positive) for the particular stage. The vertical distances on the two sides of the diagram [*i.e.* from the NaCl(s) datum to the $Na^+(g)+Cl(g)$ datum] must be numerically equal, so that

$$410+108+121+489=-(365+\Delta H_5)$$

whence $\Delta H_5=-763$ kJ mol^{-1} at 298 K.

This enthalpy change is often called the lattice energy in Born–Haber calculations. However, it should be corrected to give the true lattice energy, which is ΔU at 0 K for $Na^+(g)+Cl^-(g)\rightarrow NaCl(s)$. This correction ($\Delta H=\Delta U-2RT$) is about 8–12 kJ mol^{-1} for simple compounds, and so can usually be neglected.

In Table 3 lattice energies obtained by the Born–Haber cycle are compared with those calculated assuming the solid is essentially an ionic structure. It will be seen that there is very good agreement for the alkali halides, reasonable agreement for halides such as MgF_2 and CaF_2, but no agreement for CdI_2 where the assumption that the structure is ionic is clearly not valid.

Table 3. Lattice energies* (kJ mol^{-1})

Compound	Calculated value	Born–Haber value
LiCl	−825	−817
NaCl	−764	−764
KCl	−686	−679
KI	−617	−606
CdI_2	−1 996	−2 410
MgF_2	−2 915	−2 908
CaF_2	−2 584	−2 611
CaO	−3 485	−3 464
Al_2O_3	−15 514	−15 326

The very high values for CaO and Al_2O_3 reflect the importance of the ionic charges; the product z^+z^- in the expression for the calculated lattice energy is 4 for CaO and 6 for Al_2O_3.

* Values taken from M. P. Tosi, *Solid St. Phys.*, 1964, **16**, 54; and T. C. Waddington, *Adv. Inorg. and Radiochem.*, 1959, **1**, 157, converted from kcal mol^{-1} to kJ mol^{-1} using the conversion 1 kcal = 4.184 kJ.

Applications of the Born–Haber cycle and lattice energy calculations

Ionic character of bonding in crystal structures

Lattice energy calculations of the type described above are based on the assumption that there is an interaction between ions according to the Coulomb law. Good agreement between these calculated values and those obtained indirectly from the Born–Haber cycle therefore provides strong support for this assumption. Conversely, the fact that the two values do not agree, *e.g.* for CdI_2, indicates that the

bonding in this case has appreciable covalent character. The small doubly-charged cation Cd^{2+} has a considerable polarizing power, and it distorts the charge cloud of the large iodide ion, I^-, which has a high polarizability. These polarization effects are equivalent to a partial electron-sharing between the ions, *i.e.* the bond acquires some covalent character. This, in turn, influences the geometry of the structure. Cadmium iodide has a layer structure which is described on p 57.

Determination of electron affinities

Electron affinities are extremely difficult to measure experimentally. However, if there is good reason to suppose that a particular structure MX is essentially ionic, a lattice energy can, in principle, be calculated and the value used in a Born–Haber cycle in which energy changes are known for every stage except that for the electron affinity:

$$X(g) + e^- \rightarrow X^-(g)$$

Hess's law can then be used to obtain the electron affinity. This method has been applied with great success to a rather unusual substance—the compound O_2PtF_6—with the unexpected result that a whole new field of inorganic chemistry has been opened up. In the

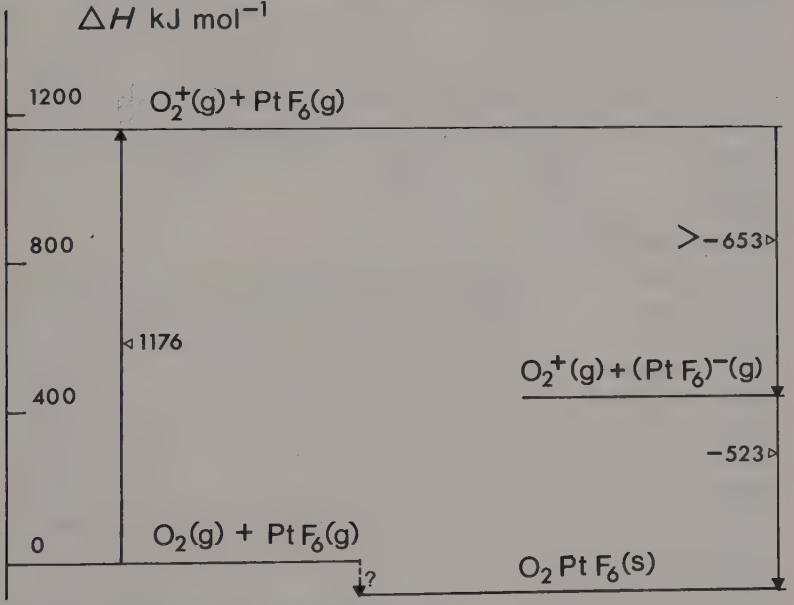

FIG. 18. The Born–Haber diagram for O_2PtF_6.

course of some work on the properties of platinum hexafluoride, PtF_6, N. Bartlett obtained the compound O_2PtF_6, a brown-yellow crystalline solid. A crystal structure determination showed that this compound was an essentially ionic structure with O_2^+ cations and PtF_6^- anions. The Kapustinskii formula was used to obtain a lattice energy of -523 kJ mol^{-1}. A Born–Haber diagram as shown in *Fig. 18* can now be constructed. There are two unknowns: the enthalpy of formation of O_2PtF_6 and the electron affinity of PtF_6. However, since O_2PtF_6 is a stable compound it seems reasonable to assume that its enthalpy of formation from O_2 and PtF_6 will be negative. The datum line for $O_2^+[PtF_6]^-$ (s) in *Fig. 18* will therefore be below that for $O_2(g)+PtF_6(g)$. Simple application of Hess's law then shows that the electron affinity of PtF_6 must be at least 653 kJ mol^{-1}. The release of so much energy in the reaction

$$PtF_6(g) \rightarrow [PtF_6]^-(g)$$

means that platinum hexafluoride is a very powerful oxidizing agent. Bartlett then used this Born–Haber diagram as a basis for selecting other substances that might be oxidized by PtF_6. A survey of ionization energy values at once revealed that the inert gas xenon has an ionization energy of 1172 kJ mol^{-1}, which is almost identical with that of O_2 (1176 kJ mol^{-1}). Xenon would not have been an obvious choice for an experiment on possible combination with PtF_6, but the Born–Haber approach revealed that it would be worth trying. The experiment was performed. An orange-yellow solid obtained immediately the two gases were mixed contained the compound $XePtF_6$ among others. This discovery initiated a period of intensive research on the heavier inert gases, and several such compounds are now known (*e.g.* XeF_2, XeF_4, XeF_6).

Stabilities of hypothetical compounds

The Born–Haber approach to solid structures is particularly useful in providing answers to questions such as: why ionic crystals are formed at all; and why sodium chloride is NaCl and not $NaCl_2$, whereas magnesium fluoride is MgF_2 and not MgF? The usual answer given in elementary accounts is that the atoms attain a stable inert gas electronic configuration by forming Na^+ and Mg^{2+} respectively. However, ionization is never an easy operation. It requires more energy to convert Mg(g) into Mg^{2+}(g) (2201 kJ mol^{-1}) than it does to convert neon into Ne^+(g) (2088 kJ mol^{-1}). Compounds of Mg^{2+} are well known; no compounds of neon are known. The thermal stability of hypothetical compounds can conveniently be discussed in terms of Born–Haber cycles, at least so far as enthalpies of formation are concerned. Strictly speaking, stability is measured by the

free-energy change (ΔG) accompanying formation of a compound from its elements in their standard states.

There may be cases where the entropy change ($\Delta S^{\ominus}$) (in $\Delta G^{\ominus} = \Delta H^{\ominus} - T\Delta S^{\ominus}$) is great enough to confer stability on a compound for which the enthalpy change is endothermic, *i.e.* ΔH positive, but in many cases a large, negative enthalpy change will imply the formation of a stable compound.

Figure 19 illustrates a Born–Haber cycle for the hypothetical ionic compound $Ne^{+}Cl^{-}(s)$. The lattice energy is computed using the

FIG. 19. The Born–Haber diagram for NeCl.

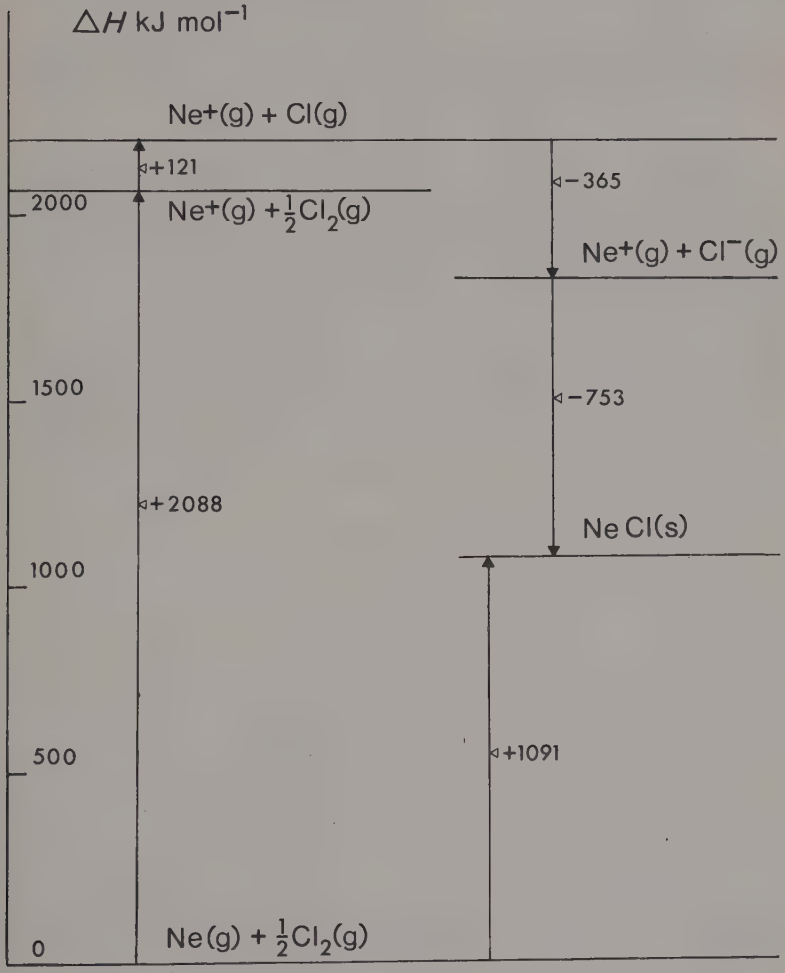

Kapustinskii equation assuming a sodium chloride type structure for NeCl and a radius for Ne^+ approximately the same as that of the neutral atom. This gives

$$Ne^+(g) + Cl^-(g) \rightarrow NeCl(s); \Delta U \simeq \Delta H = -753 \text{ kJ mol}^{-1}$$

and from the Born–Haber cycle we then get a value for the enthalpy of formation of NeCl

$$Ne(g) + \tfrac{1}{2}Cl_2(g) \rightarrow NeCl(s); \Delta H = +1091 \text{ kJ mol}^{-1},$$

i.e. an endothermic reaction.

On the other hand, a corresponding diagram for $MgF_2(s)$ gives

$$Mg(s) + F_2(g) \rightarrow MgF_2(s); \Delta H = -1100 \text{ kJ mol}^{-1},$$

so that the formation of MgF_2 is an exothermic process. The stage which is essentially responsible for the difference between the two examples is that involving lattice energy:

$$Ne^+(g) + Cl^-(g) \rightarrow NeCl(s); \Delta H \simeq -753 \text{ kJ mol}^{-1}$$

$$Mg^{2+}(g) + 2F^-(g) \rightarrow MgF_2(s); \Delta H = -2908 \text{ kJ mol}^{-1}.$$

The high value for the MgF_2 lattice energy indicates the important effect of the *doubly*-charged ion Mg^{2+} and of the Madelung constant (2.408 for MgF_2 which has the rutile structure). It is instructive to apply the cycle to the hypothetical compound MgF. If we assume that it has a sodium chloride lattice and a Mg^+ radius equal to that of Na^+ (which has the same arrangement of electrons) we get a calculated value of -904 kJ mol^{-1} for the lattice energy. This in turn leads to an enthalpy of formation of only -105 kJ mol^{-1} for MgF (s). MgF may have a transitory existence in certain circumstances, but it readily undergoes disproportionation to Mg and MgF_2, for which $\Delta H = -619$ kJ mol^{-1}.

5. A Survey of Crystal Structures

Crystal structures can be classified in a number of ways, one of which is essentially geometrical. Mathematical topology is applied to discover the possible structures that might be developed given the immediate, nearest neighbour environment of a given atom. We shall discuss some simple aspects of this approach later in this chapter (p 59) where structures are described in terms of close packing of polyhedral units, or of open packing where edges or vertices of polyhedra are shared. This classification is, however, mathematically sophisticated and not really suitable for students beginning a study of the subject. For them, a classification based on bond types seems more directly linked with chemistry. Although it must always be emphasized that descriptions of bonding in terms of extreme types of bond are very much an oversimplification, a great many structures do fall naturally into categories based on these bond types. (As is always the case, the really interesting examples are those that do not fall neatly into these categories.) We shall therefore first of all discuss structures in terms of ionic, covalent, van der Waals, hydrogen, or metallic bonds between an element and its nearest neighbour. Table 4 shows one such classification based on these bonds with a summary of the characteristic features of each type of structure.

Ionic structures

The structures of ionic compounds are determined in the main by geometrical considerations—the relative sizes of cations and anions—and by the requirement for overall neutrality. There are no preferred directions for bond formation since the electric field around simple ions is spherically symmetrical. Electrostatic theory predicts that stable structures will be those in which there is cation–anion contact with anions arranged in a symmetrical way to minimize anion–anion repulsion. The co-ordination number—the number of nearest neighbours of opposite charge in contact with a given ion—will depend on the relative radii. A co-ordination number of 12 should be possible if cations and anions have the same radii—*see Fig. 20.* Ionic structures are not found with this arrangement, however, since it is not possible to construct a regular three-dimensional array of ions in which each has a co-ordination number of 12 . If the ions are of very different sizes the co-ordination number is less than

Table 4. Classification of crystal structures

Type	Structural unit	Bonding	Characteristics	Example
Ionic	Cations and anions	Electrostatic, non-directional	Strong, hard crystals of high mp. Moderate insulators. Melts contain ions and are conductors. Some are soluble in liquids of high dielectric constant. Optical and magnetic properties are largely those of the constituent ions.	Alkali halides
Covalent	Atoms	Covalent—limited no. of electron-pair bonds, spatially directed.	Strong hard crystals of high mp. Insulators.	Diamond
Molecular	Molecules	Mainly covalent between atoms in molecule. Van der Waals (or hydrogen) bonding between molecules.	Soft crystals of low mp and large coefficient of expansion. Insulators.	Iodine; ice; crystalline organic compounds.
Metallic	Metal ions	'Metallic'; delocalized valence electron orbitals. Non-directional.	Single crystals are soft; strength depends on structural defects and grain. Variable mp. Good conductors.	Iron

12; a small cation can only accommodate a small number of large negative ions around and in contact with it. Possible co-ordination numbers in ionic crystals are often discussed in terms of the radius ratio, r_+/r_-, and many books contain diagrams of the type shown in *Fig. 21*, which shows the immediate environment of a cation in contact with six larger anions. In (*a*), the cation A^+ is in contact with six anions B^-, octahedrally arranged. If the radius ratio is now changed, in this case by keeping A^+ the same but changing to larger anions C^- or D^-, the co-ordination may change. In (*c*) the large anions D^- are in contact with each other, and not with the cation A^+. This represents an arrangement that would be less stable than one of tetrahedral co-ordination in which there was cation–anion contact. The structure AC, shown in (*b*), is a limiting case for octahedral co-ordination. The anions are in contact with each other as well as with the central cation. The limiting value of the radius

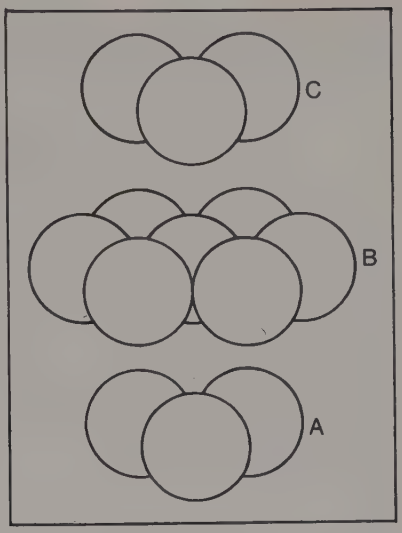

FIG. 20. Co-ordination of ions of equal radius. Each ion is in contact with six coplanar ions in layer B, with three in layer A, and with three in layer C. Layers A and C have been displaced vertically to show the geometry more clearly.

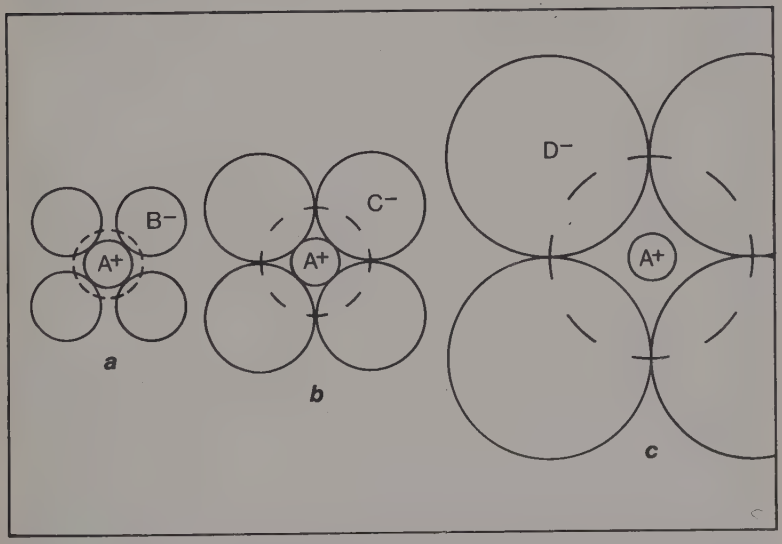

FIG. 21. Co-ordination and radius ratio r_+/r_-

ratio for any given co-ordination number can readily be calculated using diagrams of the type shown in (*b*). Table 5 gives some of these limiting values.

It is possible that this approach to co-ordination has been overstressed in recent years. Students readily grasp the relation between co-ordination number and limiting radius ratio. Ionic radii can be obtained from data books; the radius ratio is calculated and the co-

Table 5. Co-ordination and radius ratio

Co-ordination no.	Geometry	Limiting value of radius ratio r_+/r_-
8	Cubic	0.732
6	Octahedral	0.414
4	Tetrahedral	0.225

ordination number for the structure is predicted. Unfortunately, the method is normally tried out first of all on the alkali halides where it often predicts a structure different from that found from x-ray diffraction methods. Cubic co-ordination (co-ordination no. 8) should be possible for KF (radius ratio 0.98) for example but, in fact, it has the octahedral sodium chloride structure. The Madelung constants for the CsCl and NaCl structures are very similar (*see* p 28) so that the structures do not greatly differ in lattice energy, and other factors such as polarization or van der Waals forces may determine which structure is the more stable in a given case. Some substances change structure if external conditions are altered. Thus, caesium chloride has the cubic structure (described on p 43) up to 469 °C and the octahedral sodium chloride structure above this temperature. At very high pressures some potassium halides change from the sodium chloride to the caesium chloride structure type.

The radius ratio method is more successful in predicting co-ordination numbers for compounds of formula AB_2. Calcium, strontium, and barium fluorides, of radius ratio 0.79, 0.91, and 1.08 respectively, have the fluorite structure in which the cation co-ordination number is eight. TiO_2, SnO_2, and GeO_2, however, ($r_+/r_- = 0.48$, 0.51, 0.38) have rutile (TiO_2) type structures in which the cation co-ordination is six.

It is also quite easy to get involved in a circular argument. Pauling values for ionic radii are normally used (*see* p 41). These are based on structures of octahedral co-ordination, but corrections can be made for structures of different co-ordination. Thus a knowledge of the structure is needed to obtain appropriate ionic radii—which can not then be used for prediction purposes.

At present the whole topic of ionic radii is in a very unsatisfactory state. In the first place quantum theory shows that there is a finite, if small, probability of finding the electron in an atom or ion at very great distances from the nucleus. The probability or charge density function $\psi^2 dv$ has to be 'chopped off' at an arbitrary distance from the nucleus if the ion is to be regarded as a spherical charge-cloud of radius r. Nevertheless, a survey of interionic distances obtained by x-ray diffraction studies shows that ions do often behave as though they had characteristic radii in ionic structures. The difference

between the interionic distances in lithium bromide and chloride is 0.18 Å* and corresponding differences between the bromides and chlorides of Na, K, Rb, Cs are 0.16, 0.15, 0.14, and 0.14 Å respectively. This approximately constant difference can be explained if the ions are regarded as spheres of constant radius; the interionic distance is then given as the sum of the radii of ions in contact. If the value of one radius is known the value of the other can be found by subtraction, and the construction of tables of ionic radii becomes possible. For many years crystal chemists and geochemists used the tables developed by V. Goldschmidt (1888–1947), who may well be regarded as one of the founders of crystal chemistry. They were based on values of individual radii obtained by J. A. Wasastjerna using a theory that related the polarizability of an ion to its volume. Goldschmidt had himself measured interionic distances in a large number of simple compounds, and he made slight adjustments to the Wasastjerna values to get the best fit between observed interionic distances and the sums of radii.

The theoretical basis of Wasastjerna's approach is not now generally accepted, and the values suggested by Linus Pauling are often used. Pauling emphasized that the radii would be a function of co-ordination number, radius ratio, and the charge on the ion. He considered isoelectronic ions such as K^+Cl^-, and divided the interionic distance in the inverse ratio of the effective nuclear charge, *i.e.* the nuclear charge diminished by the screening effect of the inner electrons, obtaining the values $r(K^+) = 1.33$ Å, $r(Cl^-) = 1.81$ Å. This enabled him to assemble, first of all, a table of values of *univalent* ionic radii and, subsequently, values called 'crystal radii' for *multivalent* ions in structures of octahedral co-ordination. Here again values were adjusted where necessary to get the best possible fit between observed interionic distances and radii sums.

We have already referred (p 24) to recent, very precise x-ray diffraction studies in which the electron densities in some simple compounds such as NaCl have been determined. The electron density goes through a minimum along a line joining a sodium nucleus to a nearest neighbour chlorine nucleus and the position of this minimum should indicate the point at which the spherical cation and anion are in contact. Unfortunately, the radii so obtained from the results of W. Witte *et al.* are strikingly different from the Pauling or the Goldschmidt values. A new set of ionic radii has been devised by B. S. Gourary and F. J. Adrian (*Solid St. Phys.*, 1960,

* Crystallographers and structural chemists find the ångström a very convenient unit of distance ($1\ Å = 10^{-10}$ m). This unit may eventually be abandoned and replaced by the SI units—the nanometre ($1\ nm = 10^{-9}$ m) and the picometre ($1\ pm = 10^{-12}$ m).

10, 128) based on these recent x-ray diffraction results. They are shown in Table 6 with the corresponding Goldschmidt and Pauling values. It will be seen that the diffraction values give larger cations and smaller anions. Table 6 also includes a column headed *atomic radii*. These are not concerned with ionic structures but it is convenient to include them here for comparison purposes. They refer to neutral atoms, and the most recent values are obtained from computations of the radius of maximum radial charge density $[4\pi r^2 R^2(r)]$ in the outermost shell of the atom. The ionic radii of cations are considerably smaller than their atomic radii, whereas the anion radii are greater than the corresponding atomic radii.

Table 6. Ionic and atomic radii (in Å)

Ion	Goldschmidt	Pauling	Diffraction	Atomic
Li^+	0.78	0.60	0.94	1.45
Na^+	0.98	0.95	1.17	1.80
K^+	1.33	1.33	1.49	2.20
Rb^+	1.49	1.48	1.63	2.35
Cs^+	1.65	1.69	1.86	2.60
Mg^{2+}	0.78	0.65		1.50
Ca^{2+}	1.06	0.99		1.80
Sr^{2+}	1.27	1.13		2.00
Ba^{2+}	1.43	1.35		2.15
F^-	1.33	1.36	1.16	0.50
Cl^-	1.81	1.81	1.64	1.00
Br^-	1.96	1.95	1.80	1.15
I^-	2.20	2.16	2.05	1.40
O^{2-}	1.32	1.40		0.60
S^{2-}	1.74	1.84		1.00

It is interesting to note that in the early days of structure analysis W. L. Bragg developed and used a set of radii characterized by large metal ions and small anions. Later, the theories of ion polarization seemed to demand small cations and large anions. Now we have electron-density determinations from precise x-ray diffraction studies which indicate a return to large cations and small anions, although the numerical values for the radii are not the same as those adopted by Bragg. However, it is too soon to consider a general replacement of Pauling or Goldschmidt values by a set based on diffraction results. In the first place only a very small number of electron-density determinations by high precision methods has so far been completed, and the Fourier method used has serious limitations when applied to heavy atoms. The position of the electron-density minimum is also sensitive to the nature and arrangement of the surrounding ions. Thus, the minimum electron density along the calcium–fluorine line in the CaF_2 (fluorite) structure gives a Ca^{2+} radius of 0.96 Å and a F^- radius of 1.40 Å, which does not agree at all

with the F^- radius (1.16 Å) obtained from the electron density in alkali-metal fluorides such as KF. The traditional Goldschmidt or Pauling values have been of immense assistance in working out some very complex structures. The important point is that any consistent set of radii chosen to get the best fit between the sum of the radii and the measured interionic distance will be helpful in discussing solid structures. The danger lies in the uncritical and 'quantitative' use of these same radii in other situations, as, for example, in discussions of ion hydration.

We shall therefore survey ionic structures in the traditional way, assuming first of all that the relative sizes of the ions will determine the co-ordination number around the cation. Co-ordination about the (generally) larger anions is not limited by geometry except insofar as a regular three-dimensional structure must be possible. The essential limitation is that of overall electrical neutrality. In a compound of general formula MX (*e.g.* Na^+Cl^-, $Fe^{2+}O^{2-}$) neutrality requires the cation and anion co-ordination number to be the same, whereas in a compound of formula MX_2 (*e.g.* $Ca^{2+}F_2^-$) there must be twice as many singly-charged X^- ions as there are doubly-charged M^{2+} ions if neutrality is to be maintained. In this case the cation co-ordination number will be double that for the anion.

Some typical ionic structures

General formula MX

The caesium chloride structure [*Fig. 22a*]. (*e.g.*, CsCl, CsBr, CsI; NH_4Cl, NH_4Br, NH_4I;* β-brass, CuZn). Here the cation has eight nearest neighbours symmetrically arranged at the corners of a cube. Neutrality requires the anion co-ordination to be the same so that each ion in the structure is at the centre of a cubic arrangement of ions of opposite charge. The resultant arrangement is one of two interlocking primitive cubic space lattices so arranged that a unit cell corner in one lattice is at the centre of a unit cell of the other lattice. (The caesium chloride structure is sometimes called 'body-centred'. Strictly speaking this is a wrong use of the term 'body-centred' which applies to a particular type of Bravais space lattice of identical points.)

It is often useful to note the number of ions per unit cell. In CsCl there are eight ions (Cl^-) at the cube corners, but in a three-dimensional lattice each of these corners is common to eight unit cells so that the total contribution of the Cl^- ions to one unit cell is $8 \times \frac{1}{8} = 1$.

---

* These ammonium halides crystallize with the sodium chloride structure at temperatures above 457, 411, and 255 K respectively.

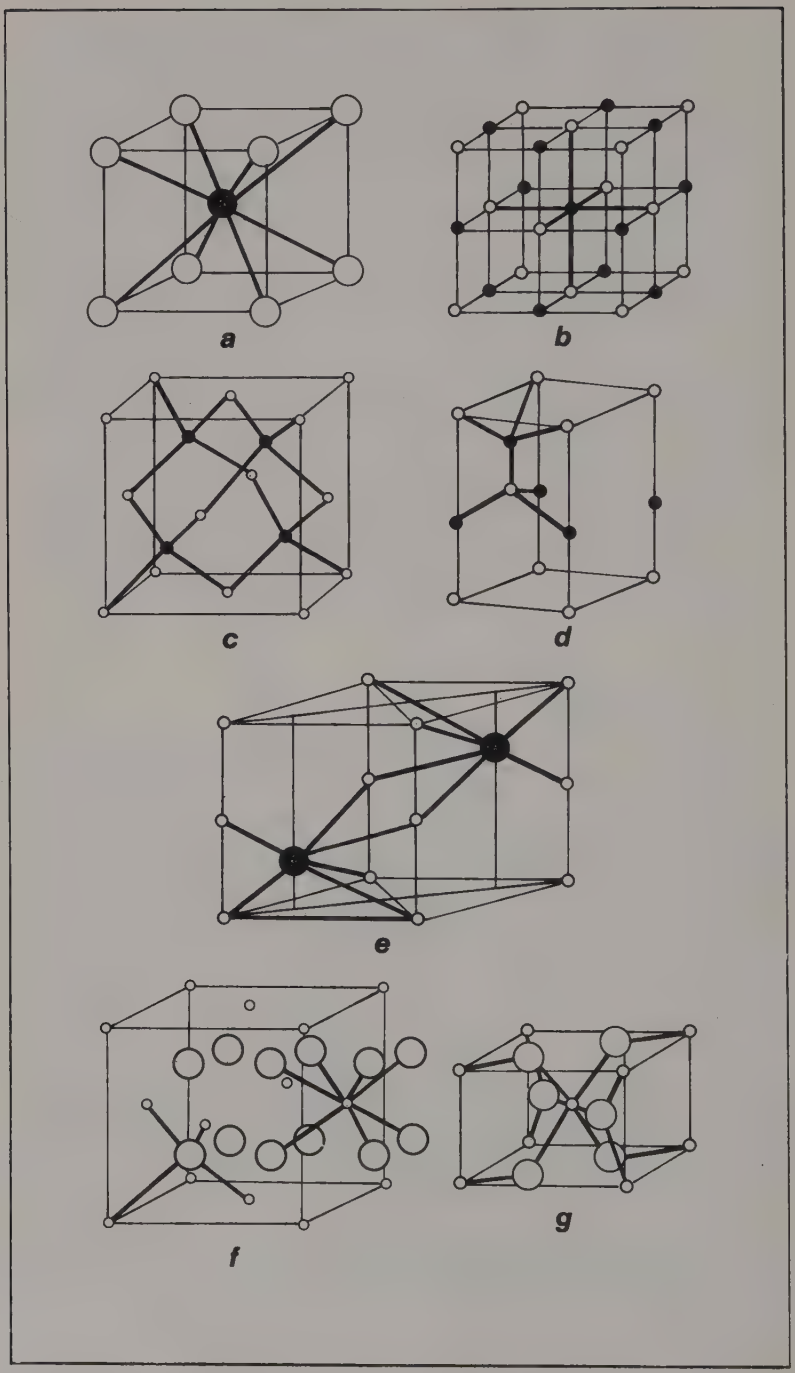

FIG. 22. Typical ionic structures (*a*) caesium chloride, (*b*) sodium chloride, (*c*) zinc blende, (*d*) wurtzite, (*e*) nickel arsenide, (*f*) fluorite, (*g*) rutile.

The Cs^+ ion at the centre of the unit cell belongs completely to that particular unit giving a total number of two ions per unit cell.

The sodium chloride structure (*Fig. 22b*). (*e.g.* alkali halides [other than Cs] and hydrides; oxides and sulphides of Group IIA metals, oxides of divalent first-row transition metals—MnO, FeO, CoO *etc.*). Each ion has six nearest neighbours of opposite charge octahedrally arranged. The structure consists of the two interpenetrating face-centred cubic lattices. For the unit cell shown in *Fig. 22b* there are four Na^+ ions (8 at cube corners shared with 8 unit cells; 6 at cube faces shared with 2 unit cells; total $8\times\frac{1}{8}+6\times\frac{1}{2}=4$) and 4 Cl^- ions (12 at mid-points of cube edges shared with 4 unit cells; 1 at body-centre position unshared; total $12\times\frac{1}{4}+1=4$).

The zinc blende structure (*Fig. 22c*). (*e.g.*, CuF, CuCl, CuBr, CuI; ZnS [blende]; CdS; HgS; MnS; GaAs; SiC). Here each ion has four nearest neighbours arranged tetrahedrally. In all structures of low co-ordination number, however, the bonding is never purely ionic. Tetrahedral orientation of electron-pair bonds is a structural feature of very many covalent compounds.

The wurtzite structure (*Fig. 22d*). (*e.g.*, BeO, ZnO, NH_4F; many of the examples quoted for zinc blende structures also exist in a wurtzite form). The co-ordination is again four for each ion, but the geometry of second nearest neighbours is different from that in the zinc blende structure. (*See* p 55 for a discussion of these structures in terms of close-packed arrangements.)

The nickel arsenide structure (*Fig. 22e*). (*e.g.*, compounds of transition metals with S, Se, Te, As, Sb, Bi). Each M ion has six nearest X neighbours at the corners of a distorted octahedron, whereas each X ion has its six M ion nearest neighbours at the corners of a trigonal prism. Each M ion also has two other M ions in close proximity and the bonding between these M ions may have considerable metallic character.

General formula MX_2

Here, as we have seen above, the co-ordination about the cation is double that of the anion to achieve overall neutrality.

The fluorite structure (*Fig. 22f*). (*e.g.*, CaF_2, SrF_2, BaF_2, $BaCl_2$; ZrO_2, ThO_2, CeO_2). Each Ca^{2+} cation has eight nearest F^- neighbours at the corners of a cube. while four Ca^{2+} cations are tetrahedrally arranged around each F^- anion.

The rutile structure (*Fig. 22g*). (*e.g.*, MgF_2, MnF_2, FeF_2; TiO_2, MnO_2, VO_2, WO_2). The radius ratio is lower for these substances (values in the range 0.38–0.72) than it is for those with the fluorite structure (0.79–1.08) so that the cation co-ordination falls to six (octahedral) arrangement. Anion co-ordination must be three (trigonal coplanar) to maintain neutrality.

Other MX_2 *structures*. When co-ordination numbers are less than six the bonds linking an ion with its nearest neighbours become increasingly covalent. Beryllium fluoride, BeF_2, has the β-cristobalite structure in which the co-ordination is 4 : 2, with a tetrahedral arrangement of anions around each cation, and a collinear arrangement of cations around the anions.

Many halides of formula MX_2 have structures similar to those of cadmium chloride and cadmium iodide, but these 'layer' structures are best discussed in a more geometrical way in terms of close-packed arrangements (*see* p 57).

General formula AX_3, A_mX_n, $A_mX_nY_p$

Here again these structures are best discussed in terms of small ions occupying interstices in a close-packed arrangement of other ions in a symmetrical way (*see* p 57).

Covalent structures

In these structures the number of nearest neighbours is determined by the number of electrons available for the formation of covalent, electron-pair bonds between atoms. The elements of Group IV of the Periodic Table—C, Si, Ge, Sn (but not Pb)—have regular three-dimensional structures in which each atom has four nearest neighbours tetrahedrally arranged (*see Fig. 23*). The C–C bond length (1.54Å) and the bond angles ($109\frac{1}{2}°$) in diamond are the same as

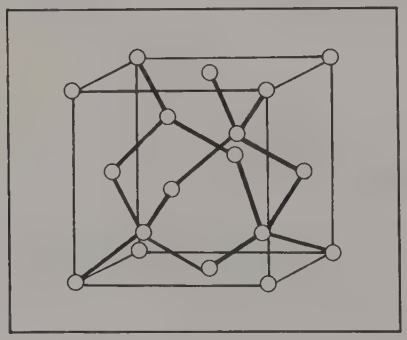

Fig. 23. The diamond structure.

those in saturated hydrocarbon chains, and a detailed electron-density determination reveals the concentration of electron charge in the region between the linked nuclei which is a characteristic of covalent bonding. These covalent bonds are strong, and structures such as diamond are hard substances with high melting points. Carborundum, SiC, and Borazon, one of the forms of boron nitride, BN, also have the diamond structure.

Molecular structures

There are very many crystals in which the presence of molecular units is revealed by x-ray structure analysis. At least two types of bonding are usually involved. Within the molecules atoms are held together by strong bonds, essentially covalent in character, but the bonds holding the molecules together in a regular three-dimensional pattern are often much weaker—either van der Waals attraction or hydrogen bonding. Some idea of the relative strengths of these bonds can be obtained from a comparison of dissociation and sublimation enthalpies. Thus for $Cl_2(g) \rightarrow 2Cl(g)$, ΔH (dissociation) = 242 kJmol^{-1} measures the energy needed to break the covalent bond linking the atoms in the Cl_2 molecule, whereas ΔH (sublimation) = 29.3 kJ mol^{-1} for Cl_2 (solid) $\rightarrow Cl_2$ (gas), is a measure of the strength of the van der Waals bond between the Cl_2 molecules in the crystal structure of solid chlorine. There are also many molecular structures in which the molecular 'unit' is extended to form long chains, or planar networks. They may be classified as follows, in terms of the complexity of the molecular unit.

Discrete molecular units (*e.g.* I_2, S_8, solid crystalline organic compounds). They usually have low melting points, since melting involves breaking the weak van der Waals bonds between molecules rather than the strong bonds between atoms in the molecule. The van der Waals bond may include a number of different contributions. If the molecule is polar there will be electrostatic interactions between dipoles, together with dipole and induced dipole attraction. Even if there are no charges or dipoles in the structure there will always be attraction between atoms or molecules arising from the 'dispersion' effect. The origin of these dispersion forces must be left for more advanced courses.

The construction and discussion of the rhombic sulphur structure can be particularly rewarding in teaching. The puckered S_8 rings illustrate the way in which covalent bond geometry, including the effect of two lone-pairs of electrons on the sulphur atoms, is determined by the repulsion of valence-shell electron pairs. The familiar, but very unusual, behaviour of the element on melting can then

readily be rationalized in terms of the preliminary breaking of van der Waals bonds between the S_8 molecules, followed by subsequent breaking of covalent bonds and ring-opening at higher temperatures. The anomalous viscosity changes result from chain growth and chain entanglement.

The units from which molecular structures are constructed need not necessarily be neutral molecules. There are many interesting chain or layer structures in which the units carry net charges, so that the inter-unit bonding, normally van der Waals, may be supplemented by ionic interactions.

Chain structures

Infinite chains, van der Waals attraction between chains (*e.g.* SeO_2, $PdCl_2$, $BeCl_2$). In selenium dioxide each selenium atom is linked by covalent bonds to three oxygen atoms. The presence of a lone-pair of electrons on the selenium atom imposes a pyramidal geometry on the SeO_3 units which are linked through oxygen atoms to form the infinite chains

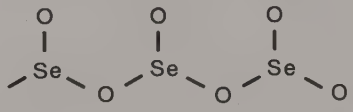

These chains are stacked together parallel to each other in the crystal structure.

The chains in palladium(II) chloride are formed by the sharing of chlorine atoms which are in a square-coplanar arrangement around each palladium atom.

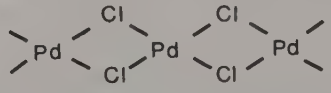

In beryllium chloride, however, the bridging chlorine atoms are tetrahedrally arranged about the metal atom in the infinite chains. These geometries are in accordance with the predictions of valency theory, and it is reassuring that structure determinations confirm the predictions.

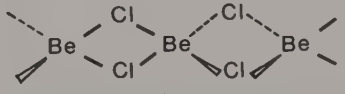

Infinite chains, ionic bonds between the chains. An example of this type of structure is $CsCuCl_3$, in which the $(CuCl_3)^-$ complex forms an infinite chain in which each copper atom is octahedrally surrounded by six chlorines. The chain structure is again the result of chlorine bridges between the copper atoms.

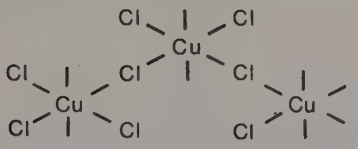

Two-dimensional network or layer structures, van der Waals bonds between layers. [*e.g.* CdI_2, MoS_2, C (graphite)]. Many chlorides, bromides and iodides of general formula MX_2 or MX_3 form layer structures.

In cadmium iodide each cadmium atom has six nearest neighbour iodines octahedrally arranged; each iodine is shared between two CdI_6 units thus building up a layer structure (see *Fig. 24a*) [*N.B.* the CdI_2 type structure is often discussed in terms of Cd^{2+} ions inserted into a close-packed structure of iodide ions (*see* p 57). The cadmium–iodine bond, however, has appreciable covalent character, and a description of the structure in terms of a molecular lattice is perhaps more appropriate].

The useful lubricant molybdenum disulphide achieves its layer structure by sharing sulphur atoms between MoS_6 units which have the geometry of a triangular prism (*Fig. 24b*).

The common form of graphite has the familiar layer structure shown in *Fig. 24c*. The stacking of the layers is such that a carbon atom in one layer is vertically above the centre of a hexagon of carbon atoms in the layer below. The layers then alternate ABABAB . . . *etc.* in the crystal structure. Graphite is polymorphic, and one of its forms has a structure in which the alternation is more complicated—ABCABCABC *etc.* This rhombohedral form is much more closely related to the diamond structure than is the common form of graphite structure.

Hydrogen bonding between layers [*e.g.* $Al(OH)_3$]. In aluminium hydroxide, and many other metal hydroxide structures, the metal ion is surrounded by six hydroxide ions in octahedral geometry. The hydroxy-groups on the underside of one layer are linked to corresponding hydroxy groups of the layer below through hydrogen bonds. (*Figs 24d* and *24e*).

Three-dimensional structures

We have already discussed the 'giant molecule' type of three-dimensional structure exemplified by ionic crystals such as sodium chloride, and covalent structures such as diamond or silicon. In these examples there is no 'molecular' unit, since the entire structure is one giant

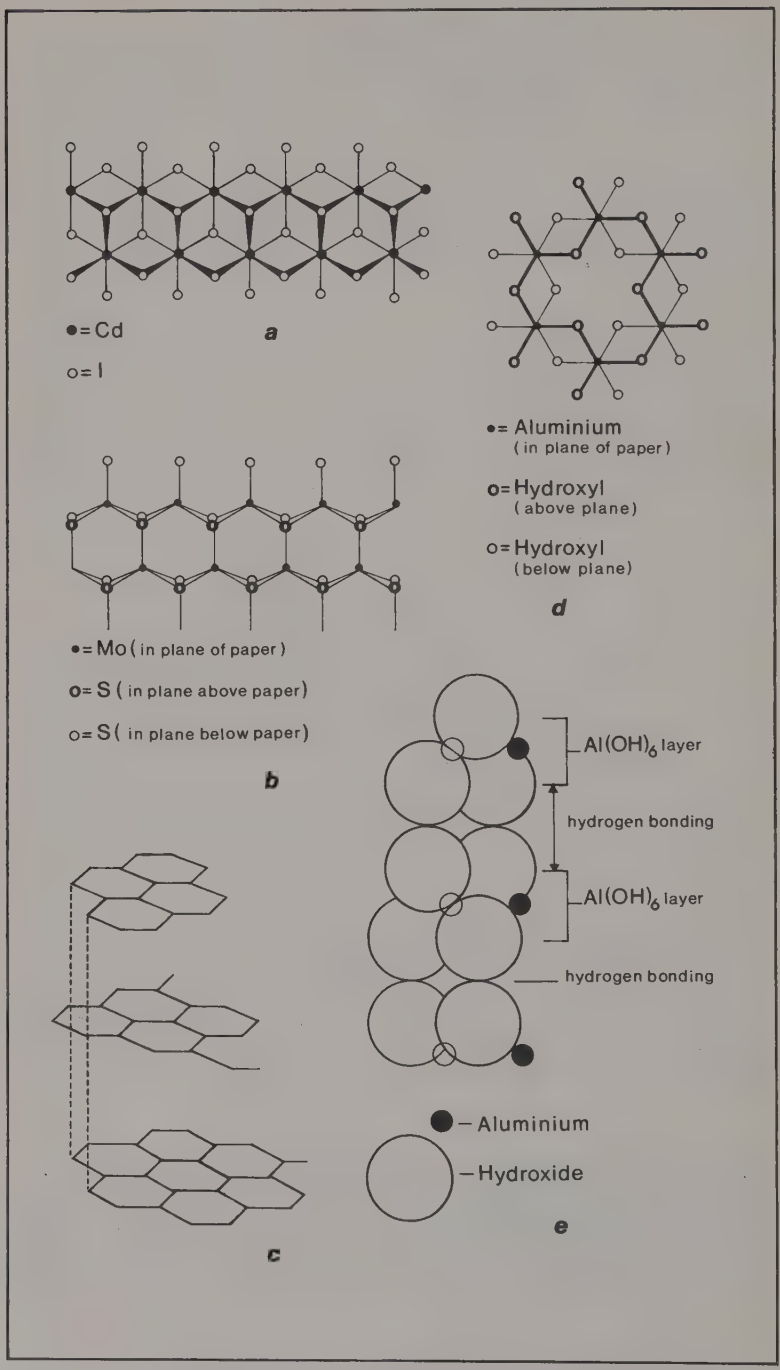

FIG. 24. Layer structures. (*a*) CdI_2; (*b*) MoS_2; (*c*) graphite; (*d*) and (*e*) $Al(OH)_3$.

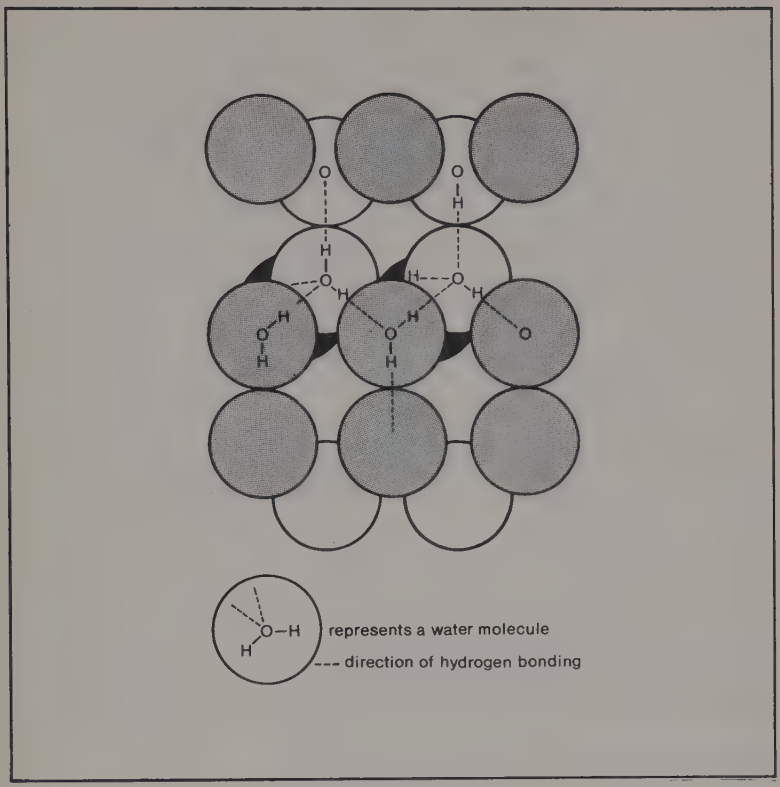

FIG. 25. The structure of ice-I.

molecule. Small molecules or complex ions may, however, link together to form a three-dimensional framework.

Ice is polymorphic. In the form obtained by normal freezing, water molecules link together through hydrogen bonds to form a hexagonal structure closely resembling the wurtzite arrangement (p 45). The form obtained by condensing water vapour on to a very cold surface, however, has a cubic structure. In each case every oxygen has four other oxygen atoms tetrahedrally arranged around it, with hydrogen atoms lying on, or nearly on, the line joining adjacent oxygens (*see Fig. 25*).

The structures of large organic molecules

The most spectacular advances in the techniques of structure analysis by x-ray diffraction have been made in the field of organic chemistry. Progress was slow in the early days because of technical

difficulties. It was impossible to locate hydrogen atoms because they gave only very weak x-ray scattering, and the important atoms, carbon, nitrogen, and oxygen were difficult to differentiate since they had similar scattering powers. Nevertheless, Kathleen Lonsdale completed the structure determination of an aromatic compound, hexamethylbenzene, in 1929; this work provided the first direct evidence for the planarity of the benzene ring.

J. D. Bernal's work on the structure of crystalline sterols also had a marked impact on experimental chemistry. His determination of the unit cell dimensions showed at once that the then accepted structural formulae for the sterols must be wrong, since molecules with these formulae would be too big to fit into the unit cell.

The pace of structure analysis of large organic molecules accelerated from the 1940s onward, largely as a result of wartime work on the structure of penicillin. Money was available to assemble a large team of workers and provide adequate computing facilities. The development of high-speed computers and automatic crystal diffractometers has changed the scale and scope of structure analysis in recent years. Structures that at one time would require months or years of work with desk computers can now be completed in weeks or months. Each of these large molecules, however, is a special case, so that crystal chemistry does not necessarily provide the correlations that have been so useful in inorganic chemistry. The structures are essentially molecular—large, very unsymmetrical molecules held together by van der Waals forces and hydrogen bonds.

Metallic structures

About 75 per cent of the known elements are metals. They have structures of high co-ordination, high electrical and thermal conductivity, with a typical surface lustre. These properties are to a large extent explained by a theory which, in simple terms, regards the structures as a close-packed array of positive ions, held in an equilibrium position by interaction with valence-shell electrons supplied by the metal atoms. However, the valence-shell electrons are not localized in electron-pair bonds between near neighbours; they enter a delocalized molecular orbital enveloping all the cations in the structure. The conductivity of metals can then be related to possible energy changes for electrons in this delocalized orbital.

From the structural point of view we have to consider the geometry of close-packed arrays of ions of equal radius, *i.e.* the method of packing which puts as many equal spheres as possible into a given volume. *Figures 26a* and *b* show two possible ways in which close packing can be achieved. In any layer, each sphere is in contact with six others whose centres form a regular hexagon coplanar with the

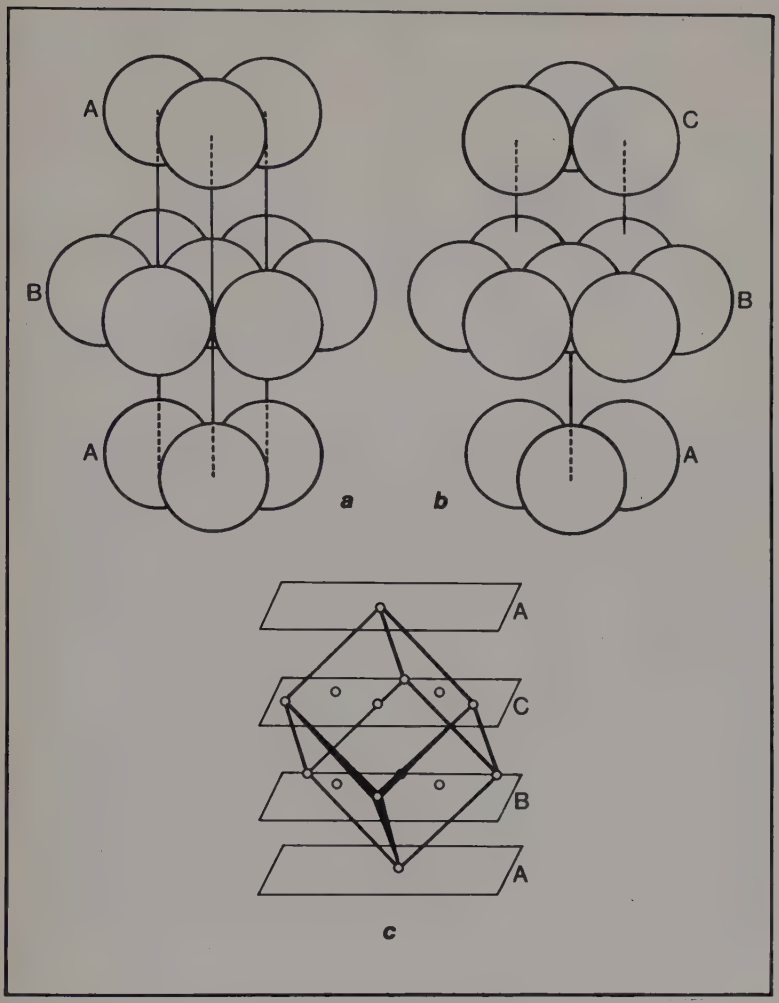

FIG. 26. Close packing of spheres.

central sphere. A second layer can now be arranged so that each sphere in layer A is in contact with three spheres in layer B. There are two different ways of adding the third layer, each of which gives rise to a close-packed structure. In *26a* each ion in the third layer is vertically above an ion in the first layer, whereas in *26b* each third-layer ion is above an interstice in layer one.

The sequence of layers in the *26a* structure can conveniently be denoted ABABAB . . . . Each ion has a co-ordination number of 12,

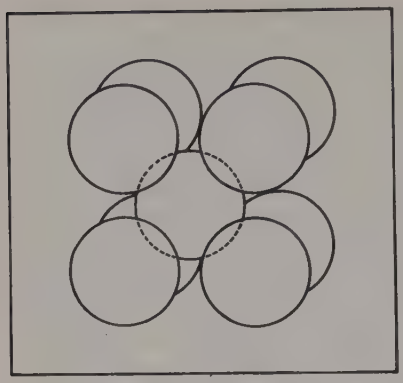

FIG. 27. The body-centred cubic structure.

and the structure has hexagonal symmetry; it is therefore termed *hexagonal close-packed*. The layer in structure *26b* can be denoted ABCABCABC . . . The co-ordination number of each ion is again 12, but the structure has cubic symmetry. *Figure 26c* shows the relationship between the parallel close-packed layers and the face-centred cube unit cell. Most metals crystallize in one or other of these two forms. There are a few which have a modified hexagonal close-packing in which the layer sequence is ABACABAC, and a few which have the body-centred cubic structure shown in *Fig. 27*. This body-centred structure is not close packed. The co-ordination number is eight, but it should be noted that there are six second-nearest neighbours at the centres of the six adjacent cubes which are not very much further away ($x_1 = \sqrt{3}/2\ x_2$, where x_1 and x_2 are the distances of first- and second-nearest neighbours from a given ion). The packing density is not very different from that of the two close-packed structures (proportion of space occupied by spheres in hexagonal or cubic close-packing is 74 per cent; the corresponding figure for body-centred cubic structures is 68 per cent). Table 7 lists some examples of the main types of metal structure.

Table 7. Metal structures

Hexagonal c.p. ABABAB---	αBe, Mg, γCa, γSr. αTi, αZr, Hf, αCo, Ni
Cubic c.p. ABCABC---	αCa, αSr, Al, Pb, γFe, βCo, Ni, Cu, Ag, Au
Body-centred cubic	Li, Na, K, Rb, Cs, Ca, Sr, Ba, βTi, V, αCr, W
Double hexagonal c.p. ABACABAC---	La, Pr, Nd, Am

It will be noted that many metals are polymorphic—a factor of considerable metallurgical importance.

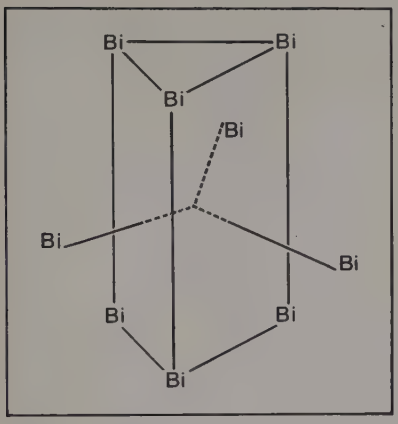

FIG. 28. The Bi_9^{5+} cluster.

The structures of metals and alloys are usually studied because of their importance in metallurgical processes. The compositions of some of the intermetallic compounds (*e.g.* $Cu_{31}Sn_3$, Ni_5Zn_{21}) pose problems for the theoretical chemist who is concerned with valency theory, but the structures are in general relatively simple. Recent work on metal 'cluster' compounds has, however, revived interest in metal bonding, and structure determinations have revealed some very interesting arrangements. In the complex rhenium anion $(Re_3Cl_{12})^{4-}$, for example, the three rhenium atoms are linked together in a triangle by metal–metal bonds in which electrons occupy delocalized orbitals. A wide range of bismuth clusters has been found in melts of bismuth trichloride in which bismuth has been dissolved. The cation Bi_9^{5+} has a structure with six bismuth atoms at the corners of a triangular prism and three more arranged above the centres of the rectangular faces of the prism (*see Fig. 28*).

Similar metal–metal bonds are found in carbonyl complexes of transition metals [*e.g.* $(CO)_5Mn–Mn(CO)_5$].

Geometrical classifications of structure

So far we have been discussing structures in terms of bond types but, as was pointed out earlier, it is sometimes convenient to use a more geometrical approach.

Structures related to close-packed arrangements

The close-packed arrangement adopted in many metal structures has been discussed (p 52). Structures which are not metallic can also be related to these close-packed arrangements: large anions may be close packed, with small cations entering the interstices

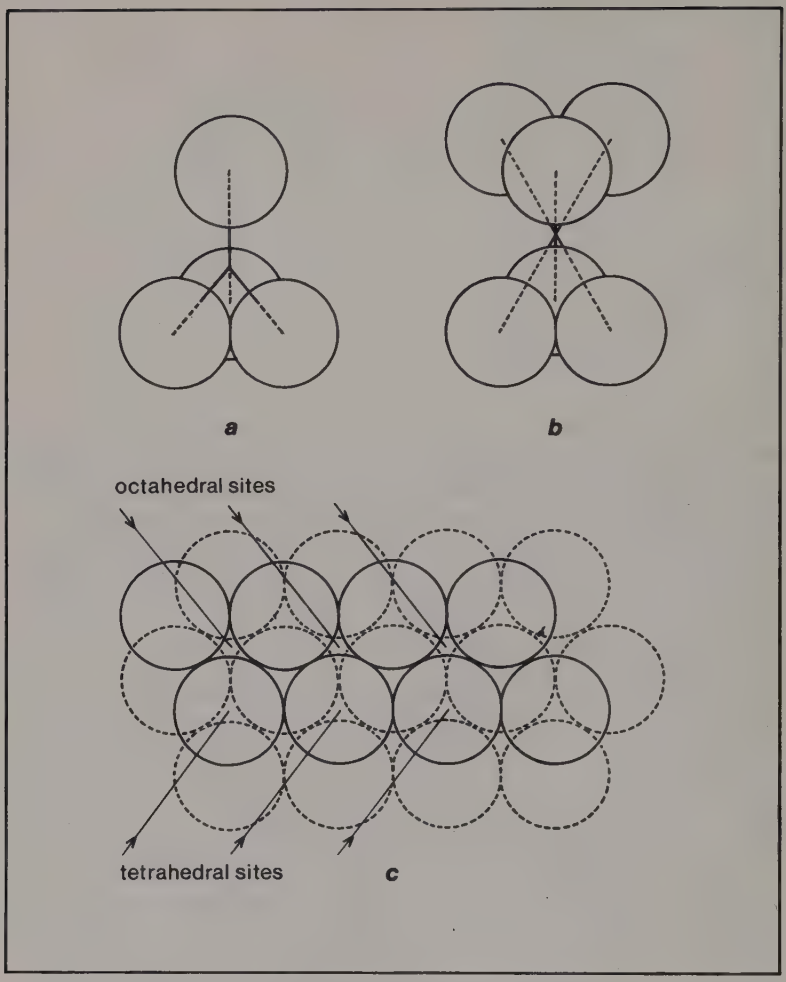

FIG. 29. Sites of tetrahedral and octahedral co-ordination in close-packed structures.

between the anions. There are two types of interstice or 'hole' into which ions may be inserted in a close packed structure.

Figure 29a illustrates a 'tetrahedral hole' or position of tetrahedral co-ordination for the ion occupying this site. It is in contact with three ions in the layer below, and one in the layer above. *Figure 29b* illustrates an 'octahedral hole'. An ion in this position is in contact with six other ions, three in the layer below, three in the layer above. The relative positions of these holes between two layers of a close-

packed structure are shown in *Fig. 29c*. Octahedral holes are larger than the tetrahedral ones. If r_+ is the radius of a cation in contact with four anions of radius r_- in close-packing, $r_+ = 0.225r_-$, whereas for an ion occupying an octahedral hole $r_+ = 0.414r_-$.

In any collection of N ions in a close-packed arrangement there are N octahedral holes and $2N$ tetrahedral holes. We can now use these considerations to reclassify ionic structures. If small cations M occupy all the octahedral holes in a close-packed arrangement of X anions we shall get equal numbers of cations and anions in the structure and a formula MX. Thus, a potassium chloride structure could be described as a cubic close-packed arrangement of chloride ions with all the octahedral holes occupied by potassium ions. It should be emphasized that in many cases the anions, although in contact with cations, may not be in contact with each other. Close-packing implies ions packed together, in contact; we can, however, still talk of 'close-packed geometry' even though the ions in the close-packed arrangement are not in contact. This distinction between close-packing and close-packed geometry is important. Thus, calcium fluoride is often described in terms of calcium ions in cubic close-packing with fluoride ions occupying all the tetrahedral sites. In this case, how-

Table 8. Structures related to close-packed arrangements

Formula	Cation: anion co-ordination	Type and number of holes occupied	Examples	
			Cubic c.p.	Hexagonal c.p.
MX	6 : 6	All octahedral	NaCl, FeO, MnS, TiC	NiAs, FeS, NiS
	4 : 4	$\frac{1}{2}$ tetrahedral, every alternate site occupied	ZnS (zinc blende) CuCl, AgI,	ZnS (wurtzite)
MX_2	6 : 3	$\frac{1}{2}$ octahedral; alternate layers have fully occupied sites; layer structure	$CdCI_2$	CdI_2
	8 : 4	all tetrahedral; cations in close packing	CaF_2, ThO_2, ZrO_2, CeO_2	
MX_3	6 : 2	X in $\frac{3}{4}$ of cubic c.p. sites M in $\frac{1}{4}$ octahedral sites	ReO_3	
M_2X_3	6 : 4	$\frac{2}{3}$ octahedral sites		α-Al_2O_3 $FeTiO_3$ (Fe and Ti in octahedral sites)

ever, the Ca^{2+} ion is smaller than the F^- ion. The Ca^{2+} ions form a face-centred cubic lattice (*i.e.* they have the geometrical arrangement that large ions in cubic close-packing possess) but they are not in contact with each other. Table 8 summarizes the way in which a large number of structures can be interpreted in terms of close-packed arrangements.

The mineral perovskite provides a name for a class of structures of general formula ABO_3 in which the A cation and the oxide ion O^{2-} together constitute a cubic close-packed arrangement. The A ions occupy the corners of a unit cell (common to eight units) and the O^{2-} ions the face-centre positions (common to two units) so that A occupies $\frac{1}{4}$ of the available sites in cubic close-packed positions. The B ion, at the centre of the unit cells, occupies $\frac{1}{4}$ of the octahedral sites (*see Fig. 30*).

Compounds such as $SrTiO_3$ and $BaTiO_3$ have this structure, but perovskite itself, $CaTiO_3$ has a distorted version of lower symmetry. It should be emphasized that structures of this general type, ABO_3, are complex oxides. There is no oxyanion unit such as TiO_3^{2-} and therefore no justification for calling the compounds 'titanates'.

Crystals with *spinel* structures have important industrial applications. The general formula for these oxide structures is $M_2^{III}M^{II}O_4$ (*e.g.* Al_2MgO_4). In the normal spinel structure (*e.g.* Mn_3O_4) Mn^{3+} ions enter octahedral holes and the Mn^{2+} ions occupy tetrahedral

Fig. 30. The perovskite structure.

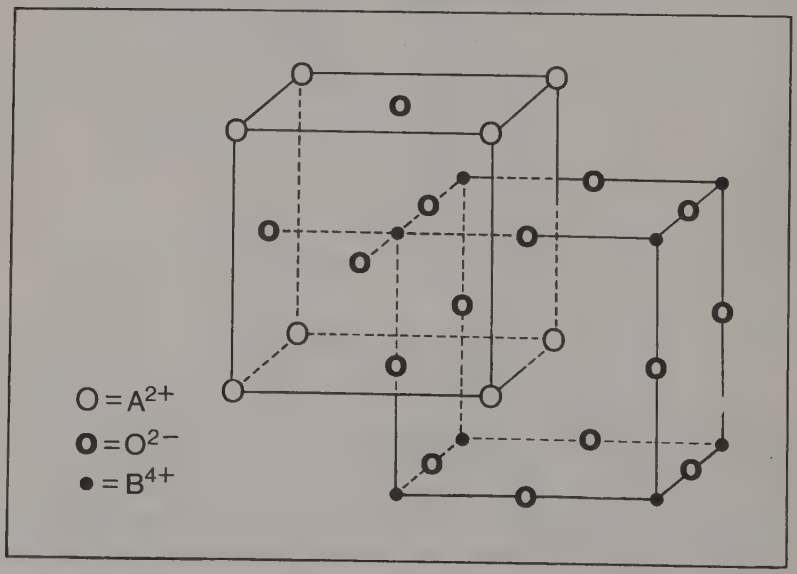

holes (even though Mn^{3+} ions will be smaller than Mn^{2+}). Only $\frac{1}{8}$ of the tetrahedral sites and $\frac{1}{2}$ of the octahedral sites are occupied. In *inverse* spinel structures the M^{2+} ions occupy octahedral sites whereas half the M^{3+} ions occupy octahedral, and the other half are in tetrahedral sites (*e.g.* Fe_3O_4, Fe^{2+} in octahedral and Fe^{3+} in octahedral and tetrahedral sites).

Silicate structures have often been discussed in relation to close packing. The Pauling crystal radii for O^{2-} and Si^{4+} are 1.40 Å and 0.41 Å respectively, so that it seems reasonable to describe many silicate structures in terms of a small cation occupying a 'tetrahedral hole' in a close-packed oxide structure. This approach is, however, misleading. Some precise electron-density determinations have been made on α-quartz and on several silicates. These show that the Si–O bond has very appreciable covalent character (*ca* 60 per cent). The bond length, Si–O, 1.62 ± 0.03 Å, is considerably shorter than the sum of the radii ($1.40 + 0.41 = 1.81$ Å), and the Si–O–Si angle is 145°. So, although a description of silicates in terms of close-packed oxide structures was extremely useful in the early days of crystal chemistry, an approach based on co-ordinated polyhedra is now more appropriate.

Structures considered as co-ordinated polyhedra

Silicate structures can be discussed in terms of tetrahedral SiO_4 units which may either exist as discrete units or else share oxygen atoms to form single or double infinite chains, rings, layers, or three-dimensional framework structures. (We shall refer to SiO_4 'units' rather than SiO_4^{4-} ions, since, as we have seen, the bonding in silicates is far from being pure ionic).

Discrete SiO_4 *units.*—*e.g.* olivine, which has the ideal formula $MgSi_2O_4$, but some of the magnesium is always replaced by iron so that the formula is expressed as $(Mg,Fe)SiO_4$.

Infinite chains (*Figure 31a*). Single chains are formed if each tetrahedron has two of its four oxygens shared with neighbouring tetrahedra. The 'repeat unit' is SiO_3, and the minerals with this structure are called pyroxenes, *e.g.* diopside, $CaMg(SiO_3)_2$.

Double infinite chains (*Figure 31b*). These occur in the amphiboles, alternate tetrahedra sharing two and three oxygens respectively. The fibrous asbestos minerals belong to this type. These chain structures are held together by bonds from oxygen to metals such as magnesium and calcium which are at least partially ionic in character.

Infinite layers (*Figure 31c*). These are formed if each unit shares

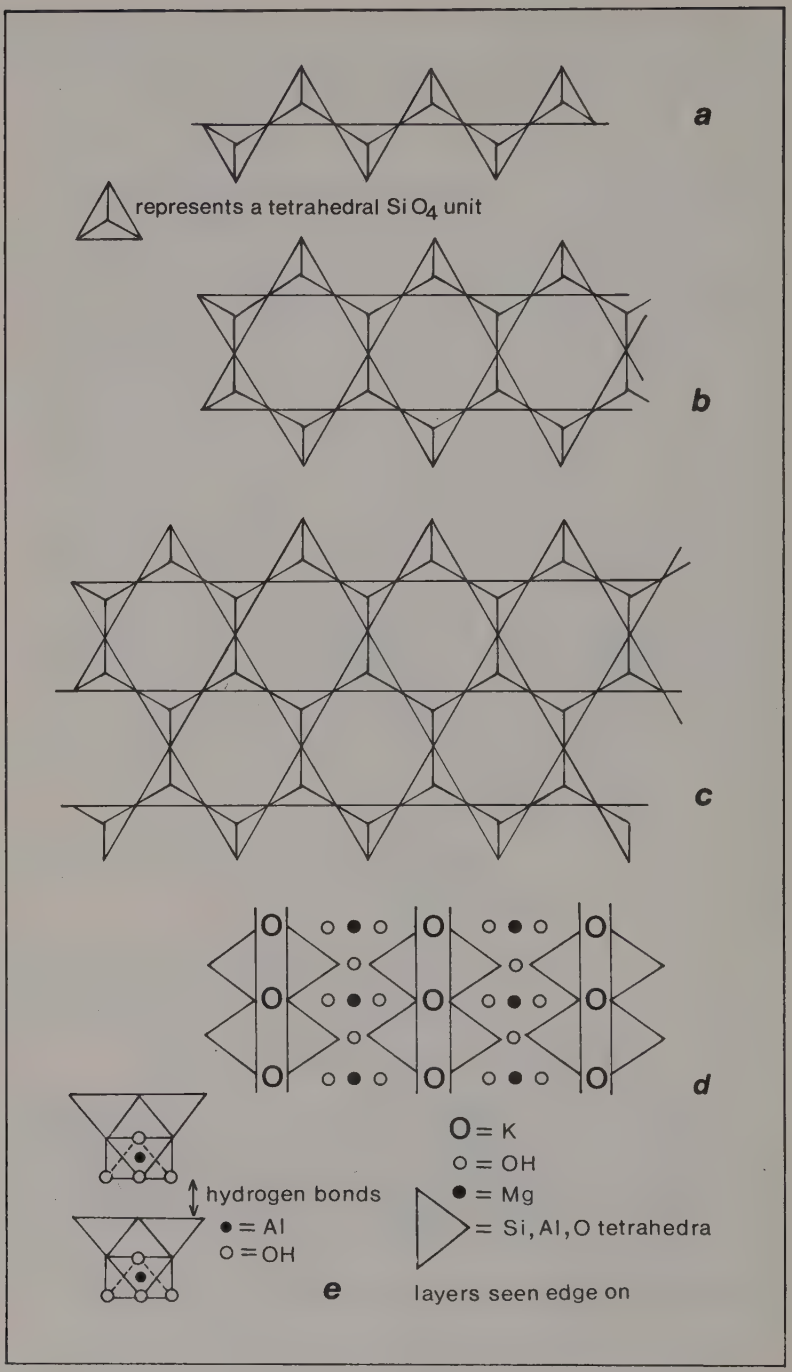

FIG. 31. Chains and layers in silicate structures.

three oxygen atoms to give a repeat unit Si_4O_{10}. The fourth oxygen atom will project either above or below the layer, and sandwich-type double layers may be formed, held together by bonds between these projecting oxygen atoms and ions such as magnesium and hydroxide. Each magnesium ion is at the centre of an octahedral unit formed by four oxygens from the silicate layers and two hydroxide ions. The sandwich units are themselves stacked together parallel to each other by weak van der Waals bonds, *e.g.* talc, $Mg_3(OH)_2Si_4O_{10}$. If one-quarter of the silicon atoms in the tetrahedral units are replaced by aluminium, the layers acquire a negative charge which can be neutralized by inserting cations between the layers. The micas belong to this structure type (*Fig. 31d*). They cleave into thin plates in a direction parallel to the layers, but the additional bonding between the composite layers makes them much harder than the talcs where van der Waals bonding only is involved, *e.g.* phlogopite, $KMg_3(OH)_2(Si_3AlO_{10})$.

Clay minerals. These are essentially single-layer silicate structures with the unshared oxygen atoms all pointing in the same direction, and incorporated into a superimposed sheet of linked $AlO_2(OH)_4$ octahedral units (*Fig. 31e*). The layers are held together by van der Waals forces.

Framework structures. These are formed if all four oxygen atoms of the SiO_4 tetrahedron are shared with neighbouring units. This can give rise to very open frameworks, as in the zeolite minerals, in which there are spacious channels and cavities that can accommodate metal ions and water molecules. Minerals of this type have been used for ion-exchange purposes and as molecular 'sieves'.

Many other inorganic structures can be described in terms of co-ordinated polyhedra. Thus, the structures of phosphorus oxyanions can be systematized by considering tetrahedral PO_4 units sharing

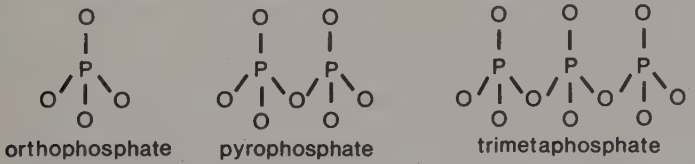

one or more vertices to form polynuclear complexes, and the complicated formulae of the polyacids of molybdenum and tungsten can also be rationalized in terms of tetrahedral or octahedral units, MO_4 or MO_6, linked together by sharing corners or edges.

6. Crystal Defects

Structure and properties

We have now discussed the way in which classical crystallography, reinforced by x-ray diffraction techniques, establishes the structure of crystalline substances in terms of a regular packing of unit cells, and we have stated that once the positions of the atoms or ions in a particular unit cell have been determined the structure of the rest of the crystal is also determined. We should, however, give a very incomplete picture of crystal chemistry if we stopped at this point. The model we have been discussing is an idealized one. It has proved to be extremely useful in correlating the properties and structures of solid substances but it fails to account for many of the properties of crystals which are so important in technology. These properties depend upon *irregularities* in an essentially regular structure.

In our survey of crystals we have drawn attention to the way in which structure influences properties. The 'giant molecule' structures are hard, have high melting points *etc.*, whereas molecular crystals are soft and have low melting points. The excellent lubricating properties of graphite and molybdenum sulphide are often associated with the ease with which weak van der Waals bonds between the layers in these structures can be broken. Unfortunately, crystal structure is often only a poor guide to the prediction of physical properties. Thus, graphite when carefully prepared in an oxygen-free environment is an extremely hard substance; its lubricating properties are presumably associated with the presence of adsorbed oxygen on the layers. A serious difficulty arises when attempts are made to calculate physical properties such as the strength or rigidity of a metal from its structure. The values obtained for the shear moduli of pure metals turn out to be about 10^5 times as great as those measured experimentally for pure metal single crystals. The weakness of single crystals arises from the movement of dislocation lines (of the type mentioned on p 18) in the metal crystal structure. Single crystals of metals, however, have to be grown by special techniques to maintain structural uniformity. Metals as normally manufactured have a 'grain' or 'polycrystalline' structure. Structure within each grain is uniform but the grain boundaries between the crystallites hinder the movement of dislocations, so that the polycrystalline material is less easily deformed than the single crystal. Alloying can greatly increase the hardness of a metal. The 'foreign' atoms tend to

congregate at grain boundaries and hinder still further the movement of dislocations in the structure. The art and science of metallurgy is thus very much concerned with defect rather than with ideal structures.

Crystal properties can be significantly modified by the introduction of controlled irregularity into an essentially regular (*i.e.* crystalline) system. The x-ray diffraction method can be used to determine the nature of these irregularities. The typical diffraction pattern is one of rows of dark spots on an x-ray film, or peaks on a diffractometer recorder, superimposed on a background of diffuse scattering. The overall or *average* structure of the unit cell can be obtained from measurements of the positions and intensities of these spots; the *shape* of the spots gives information about crystal texture or grain, since diffraction from a single crystal gives spots which have a different shape from those produced by a polycrystalline material with a grain or mosaic structure. The diffuse background gives information about thermal vibrations. The atoms in a crystal have vibrational energy even at absolute zero (the 'zero-point' or 'residual' energy), and the amplitude of these vibrations increases with increasing temperature. This means that the structure becomes increasingly irregular as the temperature rises, and the x-ray diffraction pattern becomes correspondingly more diffuse.

Lattice defects

One important type of irregularity or disorder arises from *point defects* in the crystal lattice. In some unit cells there are vacant lattice points or sites—a cation is missing from one site and an anion from another. Ions have moved to new positions on the crystal surface. The vacant sites so produced are called Schottky defects (*Fig. 32a*). Cation and anion vacancies occur in pairs so that overall neutrality and, consequently, stoicheiometry is preserved.

Frenkel defects are illustrated in *Fig. 32b*. Here ions leave lattice sites to go into interstitial positions, and neutrality is maintained when there is an interstitial ion corresponding to each vacant site. Schottky-type defects tend to be more numerous than Frenkel defects, since it is usually easier to remove ions completely than it is to force them into interstices. Cations, being in general smaller than anions, move more readily into interstitial positions, and Frenkel defects occur to a greater extent in the more open structures of the zinc blende or wurtzite type where there is more room for interstitial ions. Another factor may be the possibility of covalent bonding in the structure.

The main defects in silver chloride, for example, are of the Frenkel type, with interstitial Ag^+ ions and Ag^+ site vacancies in the

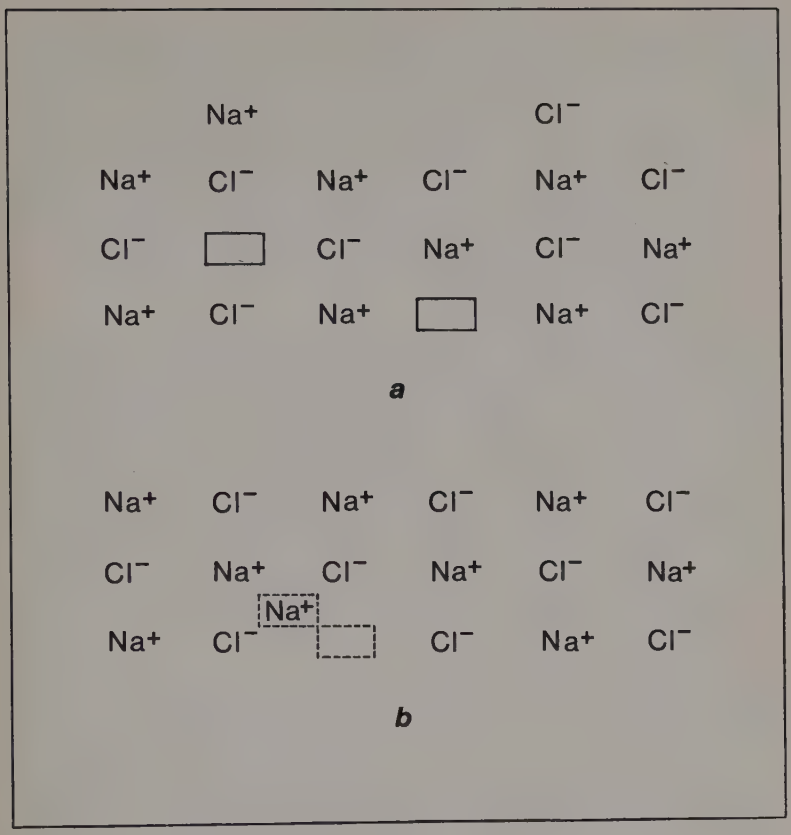

FIG. 32. Defect structures.

sodium chloride type lattice, whereas Schottky-type defects are more prevalent in sodium chloride itself. This may be due to the partial covalent character of the bond between silver and chlorine in silver chloride, which may be considerable when silver is confined in an interstitial position.

The existence of vacant sites or holes in the crystal structure provides a mechanism for diffusion of particles through the crystal. It is much easier for an ion to migrate by moving from an occupied site to an unoccupied one than to force a way through a regular array of ions in the lattice.

A convenient and important way of changing the number of vacant sites in a crystal lattice is to 'dope' the crystal with ions of different valency. If sodium chloride is crystallized from a melt con-

taining some manganese(II) chloride, Mn^{2+} ions occupy some of the cation sites in the crystal lattice. Overall neutrality is preserved if one site for singly-charged sodium ions is left vacant for each site occupied by the doubly-charged manganese cation. The introduction of controlled traces of impurities may therefore produce marked changes in diffusion rates and *ionic* conductivities in these crystals. Controlled doping is also an important method of changing the *electronic* conductivity of a crystal, but this arises from the provision of new allowed energy bands which are accessible to electrons.

Non-stoicheiometric structures

The composition of a structure containing Schottky or Frenkel defects does not differ from that of the ideal, defect-free structure. If, however, there are different numbers of cation or anion vacancies, or if interstitial ions are not balanced by site vacancies, the composition of the crystal will no longer be stoicheiometric. Different samples of the same substance may have slightly different compositions. Thus, zinc oxide can be made with a composition represented by $Zn_{1.00033}O$; there is a 0.033 per cent excess of zinc in interstitial sites in the ZnO structure. The well-known colour change from white to yellow when zinc oxide is heated arises from this excess of zinc in interstitial positions.

Nickel(II) oxide provides another example of a non-stoicheiometric compound. Black nickel oxide has an average composition $Ni_{0.98}O$, indicating that there are vacant Ni^{2+} sites in the NiO lattice. The rate of corrosion of a metal such as nickel in a dry atmosphere can be linked with defect structures. A clean nickel surface is almost instantaneously covered with oxygen when it is exposed to the gas. The O_2 molecules dissociate into atoms and strong metal–oxygen bonds are formed. Metal ions (Ni^{2+}) now diffuse from the metal surface to the oxide/oxygen interface making use of vacant sites on the way, and the rate of diffusion will depend on the number of vacant sites in the oxide layer. At the surface, newly arrived Ni^{2+} will combine to form more oxide, and the oxide layers will grow. The rate of oxide formation can be retarded by adding a small amount of lithium. Substitution of a singly-charged Li^+ ion for the doubly-charged Ni^{2+} ion leaves a net negative charge which can be neutralized by an additional Li^+ which enters a vacant Ni^{2+} site. Thus the number of vacancies is reduced and the rate of diffusion of metal through the oxide layer diminishes. If, on the other hand, a tervalent ion is added, such as Mn^{3+}, the number of vacant sites in the oxide layer must increase if neutrality is to be preserved. Such metals therefore accelerate the corrosion of nickel.

Detailed study of the defect solid state lies outside the scope of

this short survey. It is important, however, that students should not be left with a picture of a crystalline solid as a static model of perfect regularity since the technology of the solid state is very much bound up with the properties of defect structures.

Suggestions for further reading

J. G. Burke, *Origins of the science of crystals*. Berkeley: University of California Press, 1966. (History of crystallography)

F. C. Phillips, *An introduction to crystallography*. London: Longmans, Green, 1957. (A standard text on classical crystallography)

C. W. Bunn, *Crystals*. London: Academic, 1964.

C. W. Bunn, *Chemical crystallography*. Oxford: OUP, 1961.

P. J. Wheatley, *The determination of molecular structure*, 2nd edn. Oxford: OUP, 1968.

A Holden and P. Singer, *Crystals and crystal growing*. London: Heinemann, 1961. (This excellent paperback contains useful recipes for growing crystals)

R. C. Evans, *An introduction to crystal chemistry*, 2nd edn. Cambridge: CUP, 1964.

A. F. Wells, *Structural inorganic chemistry*, 3rd edn. Oxford: OUP, 1962. (The structural inorganic chemist's indispensable *vade mecum*)

N. N. Greenwood, *Ionic crystals, lattice defects, and non-stoicheiometry*. London: Butterworths, 1968.

W. J. Moore, *Seven solid states*. New York: Benjamin, 1967. (An introduction to modern solid state science)

Nuffield chemistry—handbook for teachers. London: Penguin/Longmans, 1967. (Chapter 13, Calculations from crystallographic data, contains much useful material and many excellent diagrams)

Principles of Crystal Chemistry provides an elementary introduction to the structural chemistry of solids. The first three chapters on classical crystallography, crystal growth and the discovery of x-ray diffraction provide the foundation for a more detailed study of lattice energy and the Born–Haber cycle in chapter 4.

Chapter 5 surveys the characteristic features of ionic, covalent, molecular and metallic structures and also discusses structure in terms of close-packed arrangements. The concept of ionic radius is critically examined. A final chapter emphasizes the fact that many of the important properties — and the industrial applications — of crystals are a consequence of departures from structural regularity.

E. Cartmell teaches structural chemistry at the University of Southampton where he is Deputy Director of Laboratories. He has been actively concerned with international developments in chemical education as editor of the OECD publication *Chemistry Today: a Guide for Teachers* and of the series of volumes *New Trends in Chemistry Teaching* issued biennially by UNESCO. He is the author of *Chemistry for Engineers*, now in its second edition, and co-author, with Professor G. W. A. Fowles, of the well-known text-book *Valency and Molecular Structure*.

His main interests apart from chemistry are in music and he has been a choirmaster for the past 10 years.

Price: 60p
(45p to RIC Members)

SBN 85404 018 8